

Acronym: FLARE  
Project full title: Flooding Accident REsponse  
Grant agreement No. 814753  
Coordinator: BALance Technology Consulting GmbH

---



## Deliverable 4.1



The project has received funding from the European's Horizon 2020 research and innovation programme (Contract No.: 814753)

Duration: 36 months - Project Start: 01/06/2019 - Project End: 31/05/2022

## Deliverable data

<b>Deliverable No</b>	4.1
<b>Deliverable Title</b>	Numerical Models
<b>Work Package no: title</b>	WP4.1Modelling of flooding process

<b>Dissemination level</b>	Public	<b>Deliverable type</b>	Report
<b>Lead beneficiary</b>	MARIN		
<b>Responsible author</b>	Riaan van 't Veer		
<b>Co-authors</b>	-		
<b>Date of delivery</b>	21-02-2020		
<b>Approved</b>	<b>Name (partner)</b>	<b>Date [DD-MM-YYYY]</b>	
Peer reviewer 1	Stephan Würst (BAL)	17-02-2020	
Peer reviewer 2	Spyros Hirdaris (AALTO)	19-02-2020	

## Document history

Version	Date	Description

*The research leading to these results has received funding from the European Union Horizon 2020 Program under grant agreement n° 814753.*

*This report reflects only the author's view. INEA is not responsible for any use that may be made of the information it contains.*

The information contained in this report is subject to change without notice and should not be construed as a commitment by any members of the FLARE Consortium. In the event of any software or algorithms being described in this report, the FLARE Consortium assumes no responsibility for the use or inability to use any of its software or algorithms. The information is provided without any warranty of any kind and the FLARE Consortium expressly disclaims all implied warranties, including but not limited to the implied warranties of merchantability and fitness for a particular use.

©COPYRIGHT 2019 The FLARE consortium

*This document may not be copied, reproduced, or modified in whole or in part for any purpose without written permission from the FLARE Consortium. In addition, to such written permission to copy, acknowledgement of the authors of the document and all applicable portions of the copyright notice must be clearly referenced. All rights reserved.*

## CONTENTS

<b>List of symbols and abbreviations .....</b>	<b>5</b>
<b>1 EXECUTIVE SUMMARY .....</b>	<b>6</b>
1.1 Problem definition .....	6
1.2 Technical approach and work plan .....	6
1.3 Results .....	6
1.4 Conclusions and recommendation .....	7
<b>2 INTRODUCTION.....</b>	<b>8</b>
2.1 Flooding of a damaged ship in waves.....	8
<b>3 NUMERICAL SIMULATION TOOLS .....</b>	<b>9</b>
3.1 Introduction.....	9
3.2 Description of numerical tools.....	9
3.2.1 <i>PROTEUS3 (MSRC)</i> .....	11
3.2.2 <i>NAPA (NAPA Group)</i> .....	11
3.2.3 <i>HSVA ROLLS (HSVA)</i> .....	12
3.2.4 <i>aNySIM (MARIN)</i> .....	12
<b>4 TIME DOMAIN FLOODING SIMULATION ASPECTS.....</b>	<b>14</b>
4.1 Introduction.....	14
4.2 Ship hydrodynamics for a damaged ship .....	14
4.2.1 <i>Hydrodynamics of a listed ship</i> .....	14
4.2.2 <i>Dead ship condition drifting in beam seas</i> .....	15
4.2.3 <i>Roll damping in waves</i> .....	15
4.2.4 <i>Wind loads</i> .....	17
4.3 Flood water dynamics .....	18
4.3.1 <i>Transient and Progressive flooding</i> .....	18
4.3.2 <i>Steady flow assumption (Torricelli/Bernoulli)</i> .....	19
4.3.3 <i>Compartment modelling / Air entrapment</i> .....	22
4.4 Hull breaches .....	23
4.5 Leakage and collapse of non-watertight structures .....	23
4.6 Validation, ITTC Benchmark .....	24
<b>5 CONCLUSIONS AND RECOMMENDATIONS.....</b>	<b>26</b>
5.1 Conclusions .....	26
5.2 Recommendations .....	26
<b>6 REFERENCES .....</b>	<b>27</b>



<b>7</b>	<b>ANNEXES</b>	<b>28</b>
7.1	Annex A: Public summary	28
7.2	Annex B: PROTEUS3 software	29
7.3	Annex C: NAPA flooding software	37
7.4	Annex D: HSVA Rolls software	47
7.5	Annex E: aNySIM software	60
7.6	Annex F: Hull breach	63
7.7	Annex G: Leakage and collapse of non-watertight structures	77



## List of symbols and abbreviations

<b>DoF</b>	Degree of Freedom
<b>ITTC</b>	International Towing Tank Conference
<b>CFD</b>	Computational Fluid Dynamics
<b>RAO</b>	Response Amplitude Operator
<b>TD</b>	Time domain



# 1 EXECUTIVE SUMMARY

A variety of numerical methods are available to predict progressive flooding; four of such methods are available through partners the FLARE consortium.

In this report an overview is given of the various methods used by the FLARE partners. The four models are based on the similar principles, but they are not identical. All methods do account for the non-linear hydrostatics due to the changing underwater geometry of the damaged ship. Two models solve the 6-DOF motion equations using non-linear wave excitation, one model solves a combine 2-DOF non-linear/4-DOF linear system, and one model is denoted as a quasi-static model as it neglects the ship hydrodynamic properties.

The flood water progression in the ship is based on the steady Bernoulli equation in all four models. One model solves in addition the shallow water equations to better accommodate the flow progression on large open spaces.

All calculation methods have short calculation times so that they can be efficiently used in the evaluation of damage stability survivability in waves. Only one model is commercially available, the other three models are used by the partners in their research and commercial work. All methods are well validated for that purpose. The complexity of the numerical model lies primarily in to which detail the damage geometry is defined. This affects the outcome of the simulation, and the larger objective in WP4 is to generate further inside in this matter through the model tests (WP4.2) and benchmarking (WP4.3) task.

In this report the current state-of-art of the four numerical models are presented. Next to this, general aspects of ship hydrodynamics related to damaged ships, and general and specific aspects of flood water dynamics are discussed.

## 1.1 Problem definition

- The current state-of-art of the numerical simulations tools as available through partners in the FLARE consortium is discussed.

## 1.2 Technical approach and work plan

- All partners have delivered a description of their numerical simulation tool; these are included in annex. A short summary is included in the main body of the present report.
- Aspects of ship hydrodynamics of a damaged ship are discussed.
- Aspects of floodwater dynamics are discussed.
- Aspects of leakage pressure and collapsing doors are discussed.
- Aspects of the hull breach are discussed.

## 1.3 Results

- A state-of-art review of numerical models used for damage ship time domain simulations.

## 1.4 Conclusions and recommendation

- The present numerical tools are well developed, verified and validated. Still some knowledge gaps and uncertainties do exist with respect to basic ship hydrodynamic properties as well as to the importance of flood water dynamics. The significance of these uncertainties on the final outcome of ship survivability is not yet fully understood.
- The present numerical tools are state-of-art for damage stability calculations but all models rely on the user defined input values (such as discharge coefficients, roll damping coefficients) that can affect the final outcome of the simulation.
- It is recommended that the model tests of WP4.2 provide sufficient data on the above mentioned uncertainties for the benefit of the benchmarking task in WP4.3 and in view of the improvement of numerical models and/or the application thereof for ship survivability assessments.



## 2 INTRODUCTION

### 2.1 Flooding of a damaged ship in waves

The flooding of a ship is for long known as a severe risk that could lead to capsizing or sinking and the loss of life at sea. The most tragic sinking of the RMS Titanic on her maiden voyage in April 1912 made her one of the most famous ships in maritime history and it was soon after realized that safety of life at sea could be provided by using certain design and operating standards. Two years after the Titanic disaster the first SOLAS Convention was adopted; and updated many times after.

It is interesting to note that the Titanic sank in about two hours and forty minutes after she struck an iceberg, and that it was mainly due to the improper lifesaving equipment and management that 1503 people out of the estimated 2224 people on board lost their life. Nowadays, 100 hundred years after, the topic is rightfully on the research agenda as ship designs evolve and loss of stability leading to limiting functionality of essential safety systems should be prevented by appropriate actions.

The present report is not about historic accidents and related safety matters. Other WP's in FLARE will address the latter. WP4.1, and hence this report, deals with the numerical models and the scientific approach applied in these models.

The (four) time domain simulations tools developed and used by the FLARE partners are based on similar principles but are all different in the details.

The approach in the MSRC/Brookes Bell and MARIN simulation tool is basically the same and can be described as a 6-DOF non-linear large amplitude ship motion time domain solver in combination with (quasi-steady) Bernoulli-based flood water progression through the ship.

The HSVA model solves the surge and non-linear roll ship motions in time domain (2-DOF) by considering the other 4-DOF ship motions through linear RAOs. Next to the Bernoulli based flow assumption for nearly full compartments, the flooding model solves the shallow water equations for flood water progression on e.g. large open decks. The HSVA Rolls flooding model is thereby unique and can be considered as the most advanced flooding model, in particular for application to the RoPAX case.

The NAPA simulation tool includes a (quasi-steady) 3-DOF ship motion solver in calm water conditions while neglecting the ship hydrodynamics properties (wave loads). However, the water pumping due to wave action is accounted for through the assessment of the relative motions between the hull breach and the incident wave profile.

Based on past verification, validation, research and industry application, the consensus between the users of the various numerical simulation tools is that the tools capture the relevant physics to great extent and with sufficient accuracy to support the FLARE project deliverables and objectives.

This report provides detailed information about the models; see chapter 3 and the annexes.

General and specific aspects of the numerical modelling of a damaged ship in waves and the floodwater dynamics are discussed in chapter 4 (and annex).

Conclusions and recommendations can be found in chapter 5.



## 3 NUMERICAL SIMULATION TOOLS

### 3.1 Introduction

The following four FLARE partners have developed the named numerical time domain flooding simulation tools:

- MSRC-University of Strathclyde/Brookes Bell Group: PROTEUS3
- NAPA Group: NAPA
- HSVA: HSVA Rolls
- MARIN: aNySim (MARIN's generic TD-tool; previously FREDYN was applied)

In the following sections the numerical tools are shortly introduced. Further details can be found in annexes B through E, and Volume 2 (HSVA Rolls only).

It is not the purpose of this document to present a full-blown overview of the software packages and their capabilities and functionalities.

The benchmark study of WP4.3 will report on the performance and capabilities of the different numerical tools to capture the obtained flooding of a Cruise ship and RoPAX vessel in model test experiments. This will further enhance the discussion on the different numerical approaches in the various simulation tools.

### 3.2 Description of numerical tools

A description of the numerical tools of the four contributing partners is provided in the following annexes:

- PROTEUS3: Annex B
- NAPA: Annex C
- HSVA ROLLS: Annex D and Volume 2.
- aNySIM: Annex E

The brief description/introduction of each numerical tool is given in below sections.

Table 3-1 highlights the main essential properties of the four simulation tools.

Table 3-1: Comparison of main essential properties of numerical tools

Functionality	PROTEUS3	NAPA	HSVA Rolls	aNySIM
Seakeeping motions	6-DOF time domain solver with non-linear wave excitation and non-linear hydrostatics.	3-DOF time domain solver (heave, roll, pitch) with non-linear hydrostatics.  Quasi-static solution in calm water.  No wave hydrodynamic loads.	2-DOF time domain solver for surge and roll with non-linear wave excitation and non-linear hydrostatics  +  4-DOF linear motions via RAO's (sway, heave, pitch, yaw).  Option to account for static trim.	6-DOF time domain solver with non-linear wave excitation and non-linear hydrostatics.
Flood water progression	Bernoulli flow type.	Bernoulli flow type.	Bernoulli flow type ,  +  Shallow water equation for large open decks.	Bernoulli flow type,  +  Cell-averaged momentum flow (under development).
Air compression in compartments	yes	yes	no	yes
Openings	Open or Closed  Collapsing pressure  Leakage area	Open or Closed  Collapsing pressure  Leakage area	Open or Closed  Collapsing pressure  Leakage area	Open or Closed  Collapsing pressure  Leakage area
ITTC Benchmark participation: 2000 (1 <sup>st</sup> ) 2004 (2 <sup>nd</sup> ) 2006 (3 <sup>rd</sup> )	Yes Yes Yes	No No Yes	No No No	Yes (FREDYN) Yes (FREDYN) Yes (FREDYN)

### 3.2.1 PROTEUS3 (MSRC)

PROTEUS3 has been developed over the last 20 years through continuous collaborative research and development by MSRC-University Strathclyde/Brookes Bell Group.

The program solves the 6-DOF (non-linear) ship motions in regular or irregular waves, coupled with empirical and semi-empirical models for flood water dynamics.

It is possible to include collapsing internal watertight doors based on a pressure head, to model variable leak rate flows, or to active/close an opening at specific time in the simulation.

Integrated Monte-Carlo sampling algorithm is available for random generation of collision and grounding damages.

PROTEUS3 has been used extensively in the prediction of vessel motions and survival boundaries for various ship types; from small fishing vessel, to cruise liners and large cargo vessels. It has been used in several high-profile casualty investigations to aid in understanding the sequence of events (e.g. MV Estonia, Costa CONCORDIA).

PROTEUS3 contributed to the various ITTC Benchmark studies.

Further details of PROTEUS3 numerical model, including references, can be found in Annex B.

### 3.2.2 NAPA (NAPA Group)

The NAPA Flooding Simulation tool is part of the NAPA software package. It is an alternative option for the calculation of a damage case and via Monte Carlo techniques the breach extents can be modelled to assess the survivability level of that damage case.

The ship motions are considered quasi static or alternatively a linear roll damping value can be specified with corresponding roll natural period. The 3-DOF motion equations are solved for heave, roll and pitch. The righting lever (GZ) arm is calculated for each time step based on the actual position of the ship. The wave excitation on the ship is not accounted for, neither are the other hydrodynamic loads such as wave radiation and wave diffraction effects. But the wave height next to the damage breach can be incorporated to account for the wave-pumping effect on the damage opening.

Each compartment is modelled as a single cell in which the free surface remains earth-fixed. The water height difference over each opening determines the mass flow rates through the opening. Air compression can be taken into account since this can have a notable effect on the flooding progression. Air pipes can be modelled. Discharge coefficients are user defined to account for accurate flow calculations; the default value is 0.6. Collapsing doors and varying leakage area over time can be included in the simulation, as well as open/close status of openings.

The NAPA Flooding Simulation tool has been validated with dedicated model tests, using a large scale model of a box-shaped barge and the results are extensively reported and analysed by Ruponen (see annex C for references).

NAPA contributed to the last ITTC Benchmark study.

Further details of NAPA numerical model, including references, can be found in Annex C.

### 3.2.3 HSVA ROLLS (HSVA)

The software/approach Rolls was originally developed by Söding in 1982 (see annex D for references), for investigating the capsizes of the container vessel E.L.M.A. Tres. In 1988 the program was extended by Petev (reference, see annex D) to deal with ships containing damaged compartments, where sloshing and in- and outflow of water takes place. There are several versions of Rolls as the program is used/maintained by different institutes in Germany. The core method of Rolls has not changed over time but HSVA has adopted the program in various modules. The version used by HSVA is called HSVA Rolls.

The roll and surge motions of the ship are determined with time-integration (2-DOF), all other motions (4-DOF) are obtained from linear RAO's. Non-linear hydrostatics and Froude-Krylov forces are taken into account in solving the roll motions.

The shallow water equations are solved for

For deeply submerged (smaller) tanks the water surface remains earth-fixed aligned with the centre of mass located at pre-calculated location depending on the orientation of the ship (tank-tables). At an opening between two compartments the difference in water height is used to calculate the inflow and outflow (Bernoulli approach).

To account for more realistic water flow behaviour in large open spaces with partial filling, such as a cargo deck, the shallow water equations are solved for those compartments. Glimms' method (1965) is implemented for this purpose (see annex D, Volume 2).

HSVA Rolls can deal with small changes of vessel trim that is an important feature for flooding simulations as water accumulation in the ship can (and usually will) introduce vessel trim which will consequently change the progressive flooding nature.

The HSVA Rolls program has been used for several investigations on passenger ship safety for IMO, for the investigation on the MV Estonia accident, as well as for other ship types such as an accident investigation for a workboat. HSVA Rolls was not included in the ITTC Benchmark studies.

Further details of HSVA Rolls numerical model, including references, can be found in Annex D.

A comprehensive description of the program is given in Volume 2 of D4.1 (this deliverable).

### 3.2.4 aNySIM (MARIN)

Around 1990, the development of a 6-DOF non-linear time domain solver in which seakeeping and manoeuvring equations were combined started in the so-called Co-operative Research Navies (CRN); led by MARIN. The program was called FREDYN, as the navy frigate (fregat in Dutch) was the main ship type of interest. A dedicated (and confidential frigate) manoeuvring model was combined with a (standard) 6-DOF seakeeping solver based on 2D strip-theory. The navies of several countries joined effort with the objective to use FREDYN for goal-based stability regulation assessment and development. The theory manual of FREDYN remains confidential and only limited description of FREDYN is reported in literature (see annex E for references).

Around 2000 a first flooding module was implemented in FREDYN based on the Bernoulli flow between compartments. It utilized pre-calculated tank-tables to define the centre of mass properties of floodwater in each compartment, assuming an earth-fixed water surface in each compartment.

In later years, the damage stability research at MARIN was extended to other ship types such as Cruise Ships in various EU funded research projects as well as for IMO developments within SLF. Time-to-sink was studied and reported (see annex E for references). This research was done using FREDYN (at zero speed when manoeuvring loads are not of interest).

Recently, all time-domain seakeeping tools developed at MARIN for various purposes are migrated to a uniform development platform called XMF. One of the more generic large amplitude time domain 6-DOF ship motion solver is aNySIM. aNySIM is restricted to zero forward speed, and was originally developed for the offshore market. Its pre-processor is a 3D panel code.

In advance of the FLARE project, motivated by limitations in the present flooding module of FREDYN, a different flooding model was developed based on a 3D cell-averaged momentum balance in combination with 1D flow between compartments. The model was denoted as UIF model (Unified Internal Flow model) and it utilizes (STL/OBJ) geometry objects instead of tank-table data. This allows for a much more robust and user friendly interface. For the FLARE project the last upgrades of the UIF model are made.

This UIF flooding model can be executed in two different modes: a) the more traditional Bernoulli type of flow progression and, b) a flooding model based on the 3D cell averaged momentum balance. Using this last option, an oscillating moon-pool, motion in an U-type anti-roll tank or even a dam-break flow were simulated. Results are not reported in literature yet. On particular motivation for the further development of the cell-averaged momentum balance method is to capture the shallow water progression in large open spaces. The first results of the model are encouraging.

Air compression in compartments can be modelled. Discharge coefficients are user defined per opening. Collapsing openings can be accounted for.

FREDYN contributed to the various ITTC Benchmark studies. aNySIM has not been validated for damage stability simulations yet, but the core hydrodynamics of FREDYN and aNySIM are identical (as they are both using the XMF framework).

Further details of aNySIM/FREDYN numerical model, including references, can be found in Annex E.



## 4 TIME DOMAIN FLOODING SIMULATION ASPECTS

### 4.1 Introduction

In this chapter several aspects related to time domain flooding simulations are discussed. The objective is to discuss the aspects considered important for the scope of work in WP4.2 (model tests) and WP4.3 (numerical benchmark study).

The following aspects will be discussed:

- Ship hydrodynamics; section 4.2
- Transient and progressive flooding; section 4.3
- Hull breaches; section 4.4, annex F
- Collapsing doors; section 4.5, annex G

The section 4.4 and 4.5 are written by HSVA and NAPA, respectively.

### 4.2 Ship hydrodynamics for a damaged ship

#### 4.2.1 Hydrodynamics of a listed ship

The state-of-art (6-DOF) time domain simulation tools are typically based on: non-linear wave excitation (Froude-Krylov), non-linear hydrostatics, linear wave radiation loads via convolution integral technique, and, linear wave diffraction through the use of RAO's.

The above mentioned non-linear wave excitation and restoring is commonly implemented in many seakeeping codes as the hull wetted geometry is easily obtained using e.g. a 3D panel representation of the hull. Most numerical tools use the undisturbed wave profile as wet-dry intersection, which is the most important change compared to calm water. The additional effect of the wave diffraction and radiation on the wet-dry hull intersection is considered to be a second order contribution.

For a damaged ship the ship hydrodynamics will change over time as the accumulated water leads to an increase of the ship displacement and a slowly varying mean list and trim in combination with wave frequent motions. All non-linear load components do account for the changing properties of the ship, but all linear components don't. All linear load components are typically established only once, in the pre-processing step for the time domain, either for the intact ship or for an a-priori defined typical damage condition. Some alternative methods have been investigated that describe the ship motions by the combination of slowly varying mean orientation in combination with wave frequent variations. It has not lead to a new uniform advocated approach, most likely since there is a stronger effect from the combined interaction between the flood water and the ship motions. A good starting point for further reading is the summary paper by Papanikolaou (2007) and the various papers presented at the International Ship Stability Workshops and Int. Conf. on Stability of Ships and Ocean Vehicles.

In-house research by MARIN (within the Cooperative Research Ships project SHIPSURV2) has shown that the hydrodynamic coefficients do change with the heel/trim of the vessel, but not always in a consistent manner over the range from intact to final equilibrium damage. The vessel RAO's did change to lesser extent than the ship hydrodynamic coefficients. The research was thereby inconclusive.

Most research seems to conclude that the changing ship hydrodynamics over time due to the sinkage and list or trim from the damaged ship are of secondary importance compared to the effect of flood water mass on the ship motion. The increased ship mass can significantly increase the roll natural period so that roll motions of a damaged ship tend to decrease compared to those of the intact ship; Gao and Vassalos (2015). This has consequence for the ingress/egress of flood water over time in irregular waves in particular.

The roll damping aspects are discussed in section 4.2.4.

#### **4.2.2 Dead ship condition drifting in beam seas**

The typical "design" damage stability assessment is performed in beam seas condition at zero forward speed. For accident investigations this might be different, but even if an accident occurs while sailing at speed, the ship's speed will soon after decrease to zero. A ship without propulsion will naturally turn towards beam seas condition.

To achieve and maintain a beam seas condition in numerical simulations it might be necessary to apply a horizontal soft-mooring system, as it is usually done in model testing. When the spring stiffness is selected well, they will not influence or suppress any of the 6-DOF ship motions due to waves. The springs, if connected to an earth fixed point, will prevent the ship from free drifting with the waves. To which extent this changes the water ingress/egress is not known, but the overall effect on the ship survivability is expected to be low, at least in a statistical sense. An alternative test set-up is to use the springs only to control the mean yaw motions and to move the towing tank carriage with the mean drift speed of the ship model. Both model test set-up configurations were applied in the EU HARDER project, but no conclusive results could be obtained of the effect of the drift velocity on the time derivative of the slowly varying ship condition.

For the benchmark study it will be important to know the exact location of the vessel in the wave field, and to know the undisturbed wave train (regular/irregular waves) so that deterministic validation is within reach.

#### **4.2.3 Roll damping in waves**

As defined in the description of the numerical tools used by the FLARE members, the roll damping of the vessel due to bilge keels is taken into account by the empirical method of Ikeda, or roll damping coefficients are prescribed. It is expected that this uncertainty will influence the outcome of the benchmark study (see conclusions from the ITTC benchmark studies, section 4.6).

It is therefore essential to provide sufficient "roll damping knowledge" from the model tests to reduce the uncertainty in the benchmark as much as possible.

At zero forward speed the main roll damping will come from the bilge keels. The flow velocity over lifting devices is absent and they will not produce any significant damping. If fins are present in the design of the ship (usually the case for cruise ships) they should not be modelled in model tests experiments (condition with retracted fins).

Typically, roll decay tests and forced roll motion tests in calm water provide a good basis from which roll damping coefficients can be obtained. These tests should be executed for both the intact as well as damaged ship condition; ideally with a closed hull breach as to establish the “listed” roll damping characteristics without any interference from the ingress/egress of water. This might be a difficult constraint for the model tests since the mass properties of the vessel should ideally be known.

When damaged, the ingress/egress of water near the damage opening will (strongly) contribute to the damping. Using CFD for the flood water dynamic in combination with a ship motion solver (PROTEUS3) lead to interesting results, although computational effort was significant, see Figure 4-1 taken from Gao, Gao and Vassalos (2011) which shows the roll response while damaged in irregular waves.

Results were presented on the roll decay simulations by Gao and Vassalos (2011) using the same coupling between a CFD solver and ship motions. A strong coupling between roll and sway was observed, as well as a strong effect from the initial heel towards or away from the damage.

There is certainly a knowledge-gap on the roll damping characteristics of a damaged ship, and in particular of a damaged ship in waves when water ingress/egress is more significant than in calm water conditions. It is recommended to further investigate these aspects in the FLARE project in the model test phase, as it will serve the benchmark task to great extent.

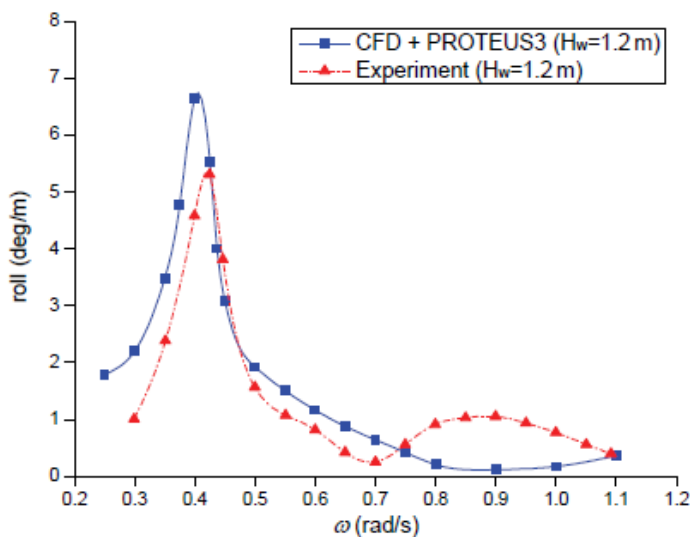


Figure 4-1: Comparison of roll RAO of PRR1 in damaged condition. From Gao, Gao and Vassalos (2011)

The effect of the drift velocity on the roll damping is demonstrated in Figure 4-2 which is taken from a MARIN in-house research project on stability of container ships. Using a constant wind force modelled by means of a constant tension winch, a mean drift velocity of 2.6 knots was obtained in upright condition. The roll decay test executed under that drift velocity indicates a significant increase of the roll damping at small motion amplitudes. The figure demonstrates the need to further research the roll damping properties under realistic conditions. It will be difficult, but perhaps not impossible, to execute roll damping tests for a damaged ship while drifting.

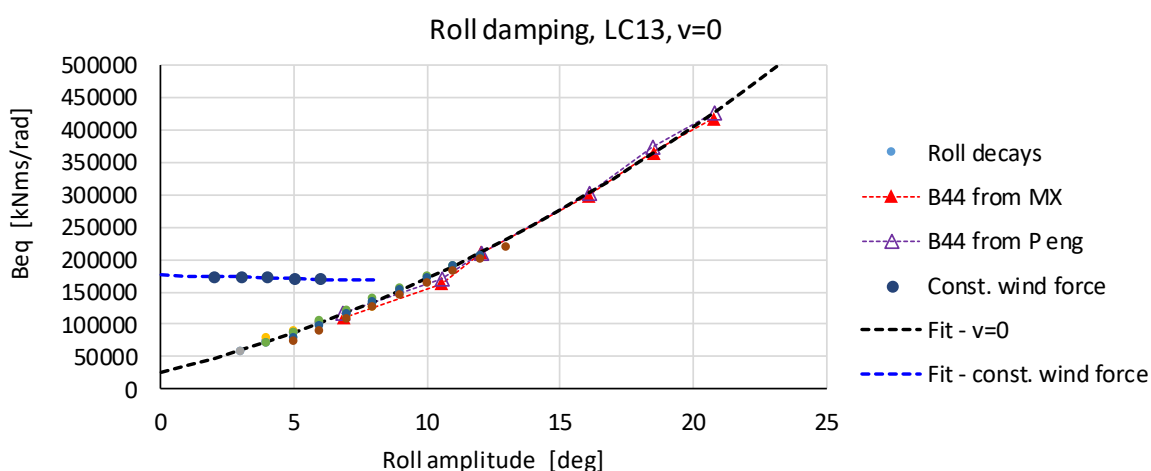


Figure 4-2: Equivalent damping of a Container ship for an intact condition. Forced roll motions are executed and the derived damping is indicated by the triangles (two different analysis methods). The roll damping while the ship is drifting in calm water at 2.6 knots is indicated by "Fit" and it is significantly higher than without drift. (from MARIN research)

#### 4.2.4 Wind loads

In numerical simulations on damaged ships, wind loads are often neglected or they are modelled using empirical coefficients (crude approximation) or coefficients based on wind tunnel tests (considered for the ship at hand). Together with a specified wind velocity, or wind spectrum, the wind loads can then be calculated.

Different databases exist in literature for various ship types and with different expected accuracy. Some references can be found in the annexes, but they refer to ships in upright condition.

The effect of heel on the wind loads is often taken into account by a  $\cos()$  reduction. This is an approximate method valid at small angles. At large heel angles wind tunnel test would be required as the nature of the flow around the vessel can change significantly. For offshore application with e.g. semi-submersibles this is daily practise.

On the other hand, for a damaged ship the wind loads are not considered very important. The general consensus is that a damaged ship will heel towards the damage and hence towards the wind force, so that inclusion of the wind load is expected to decrease the heel angle.

Therefore it is considered conservative to exclude wind loads since this will slightly increase the roll motions and vessel exposure to progressive flooding. Further discussion can be found in Papanikolou (2007).

## 4.3 Flood water dynamics

### 4.3.1 Transient and Progressive flooding

A simplified description of the flooding of a ship is captured by what is called transient and progressive flooding stage, see Figure 4-3.

Transient flooding is defined as the first phase after damage in which a large amount of water floods into the ship. It can result in violent water flow with many dynamics involved. It can lead to high pressure loads on construction details due to water impacts and subsequent damage of these impacted structures. During transient flooding large heel angles can be obtained. The wave dynamics are most likely of secondary order, that is, the heel is mainly the result of the heeling lever of the flood water ingress and its dynamics. See e.g. Figure 4-4 from De Kat and Van 't Veer (2001). Note that this is just an example and might not be generally valid in all conditions.

Progressive flooding is defined as the second phase after transient damage in which the water ingress is slow and less violent. The main water ingress will be due to the wave pumping effect near the damage opening. Still, due to a slow change of heel angle over time, progressive flooding can take place as well in calm water condition.

An equilibrium mean floating condition can be reached, the steady state, in which ingress of water does not accumulate anymore. In the worst case a capsizes occurs.

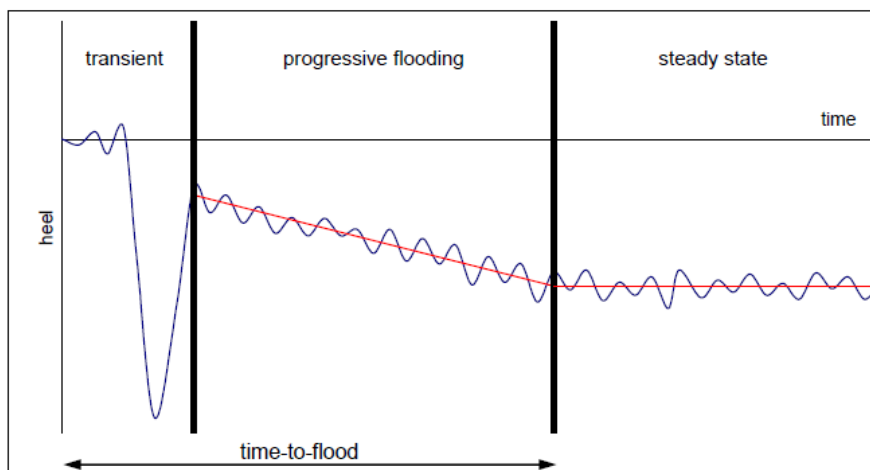


Figure 4-3: Different stages of flooding, simplified to three stages. From Ruponen (2007).

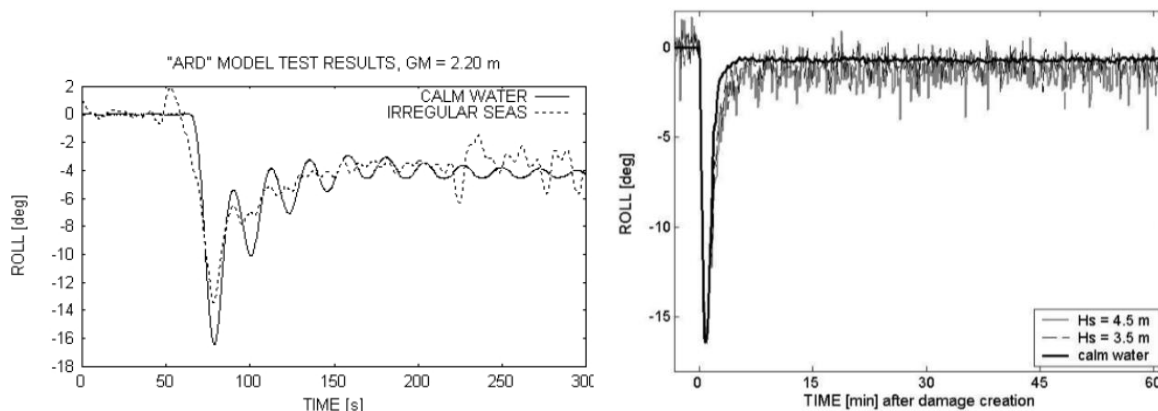


Figure 4-4: Comparison of roll response in calm water and irregular waves. Left: RoRo vessel from De Kat and Van 't Veer (2001); Right: Cruise Ship from Van 't Veer and Serra (2003)

### 4.3.2 Steady flow assumption (Torricelli/Bernoulli)

The fast time domain simulation tools all apply a quasi-steady flow behaviour in which the free surface in tanks remain earth-fixed over time; following the derivation of Torricelli (1643) or more general Bernoulli (1738). This type of flow is a classic example in fluid dynamics and hydraulics. The equations can be found in the program description in the annexes.

The coupling with a CFD tool for the flood water progression remains out of reach for practical application given today's computational power (Gao et al (2011)).

To "match" the outcome of the simple (hydraulic) equations, that neglect the flow momentum in the tank and viscous losses at the openings between floodable space, the so-called discharge coefficients are introduced. There are numerous references that list values for different opening shapes and size of such orifices. A typical value is often taken as  $C_d = 0.6$ . Only for Reynolds numbers  $Re < 10^4$  there can be important scale effects on the flow through orifices. Model tests at scale 1:50 of a 300 m vessel are feasible without too much scale effects using typical door-size openings.

It is recommended to provide discharge coefficients for the openings on model scale as is for example reported in Ruponen (2007). Care should be taken how the discharge coefficient is defined, but it is typically defined as the coefficient that reduces the flow rate  $Q$  through the damage opening with area  $A$  and with water level different  $dH$  over the opening, given by:

$$dQ(t) = C_d A v = C_d A \sqrt{2g(dH)} \text{sign}(dH)$$

The Torricelli flow velocity in the equation (above) is determined from the water height difference between the left and right compartment over an opening. Vertical openings (down/up-flooding through decks) require some special attention as well as the inclusion of air in compartments that modify the maximum filling of the compartments.

It should be noted that discharge coefficients are defined to account for frictional losses with respect to a theoretical flow velocity prediction, that is the assumption that there is no flow inertia in the tank; the Torricelli-law. To determine the discharge coefficient for a specific geometry, a large tank volume is used in combination with a relatively small orifice. Comparing the theoretical time required to empty the tank between two fluid levels with the time delta measured in the experiment, the discharge coefficient is found. Such an experiment could be executed in CFD nowadays as well. In the past many physical experiments were conducted, and coefficients are published, see e.g. Idel'chik (1960) or Bos (1989).

Entrapped air in a certain compartment can have significant influence on the final outcome of a flooding simulation. It will be complicated, even impossible, to model the real ship in numerical simulations as the ventilation properties and behaviour are difficult to define precisely. It is one of the largest uncertainties in damage stability assessments through numerical simulations. However, proper validation of the numerical tools is feasible as in model tests the ventilation properties (pipes/channels) are known precisely.

The use of CFD in the FLARE project will be limited or absent. External partners might use CFD and contribute via the benchmark study to the WP4.3 outcome, but that remains unknown at the moment. CFD might be useful to generate simple validation cases so that fast and approximate simulation tools could be benchmarked, and "calibrated" if necessary. A simple example is presented in Figure 4-5 and Figure 4-6. A three compartment model is used consisting of two cabins (C1 and C2) and a corridor (alley) connecting them. In the COMFLOW-CFD simulation (done at MARIN) a violent flow behaviour is observed, although this is less observed for the emptying compartments. The violent flow behaviour in the first 18 seconds of the simulation can never be captured by the steady Bernoulli flow models. But after the 18 seconds (full scale configuration of a cabin layout, filling was 2.5 m at the start), the flow behaviour is much more "steady".

As can be observed in Figure 4-6, there is an almost excellent agreement between the simple steady calculations based on Torricelli law and the unsteady COMFLOW simulation; in this case the  $C_d = 0.6$  was used on both openings. The differences occur in the filling of compartment C2 that starts later in COMFLOW due to the flow inertia effects in the corridor (alley). The averaged fluid level in the alley is as well somewhat different, but that could be expected having seen the violent motions in the CFD simulation.

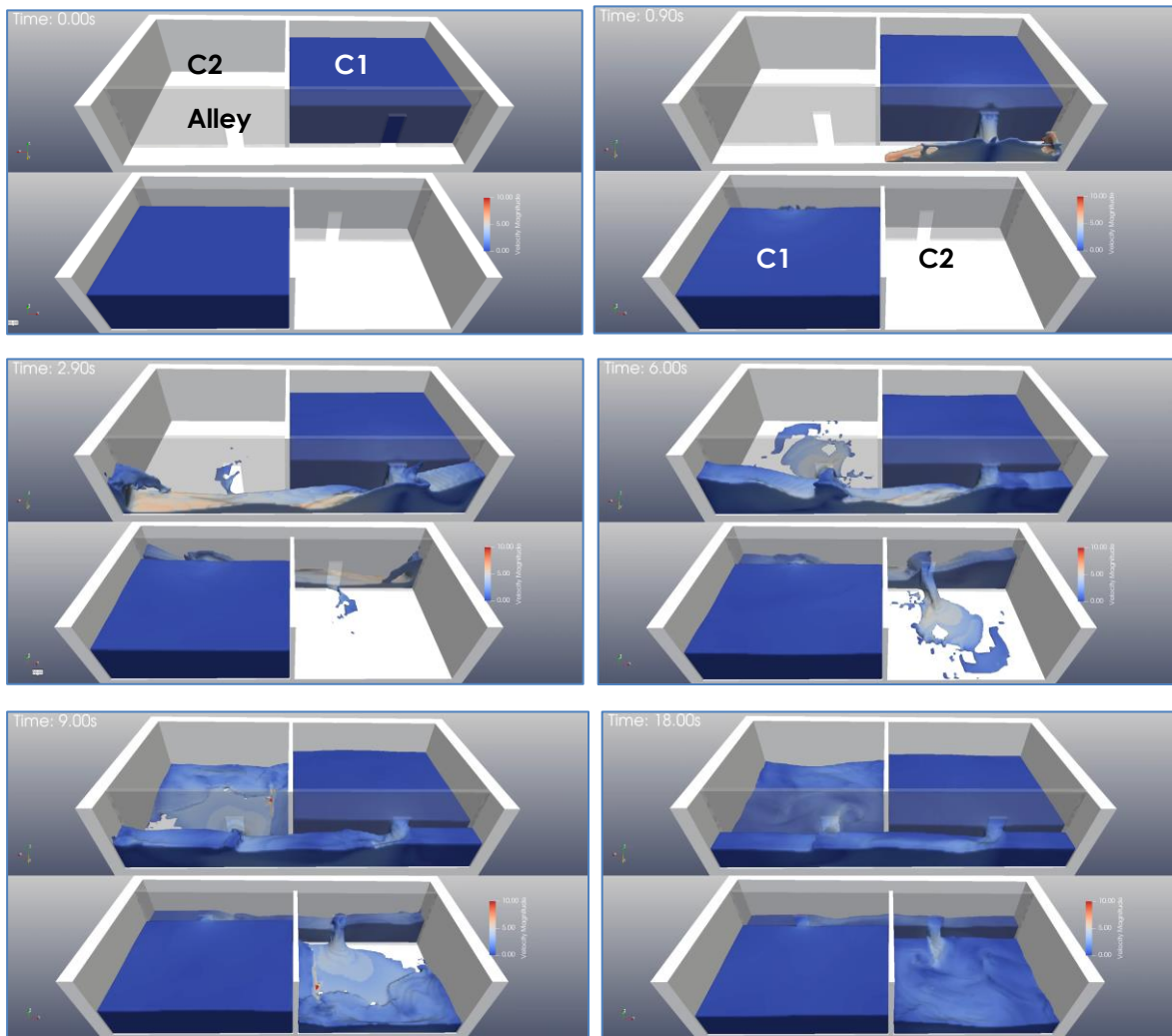


Figure 4-5: COMFLOW (CFD) simulation of a three compartment flooding (C1 is full at  $t=0$ , C2 and Alley are empty at  $t=0$  s). Snapshots at time = 0.0, 0.90, 2.90, 6.0, 9.0 and 18.0 s after 'door damage'. The dam-break type of flow is seen, collapsing on the opposing wall in the corridor, leading to violent flow behaviour, especially in the corridor. Compartment C1 gradually empties, C2 fills up in a rather complex manner with strong local variations. MARIN research (not published yet).

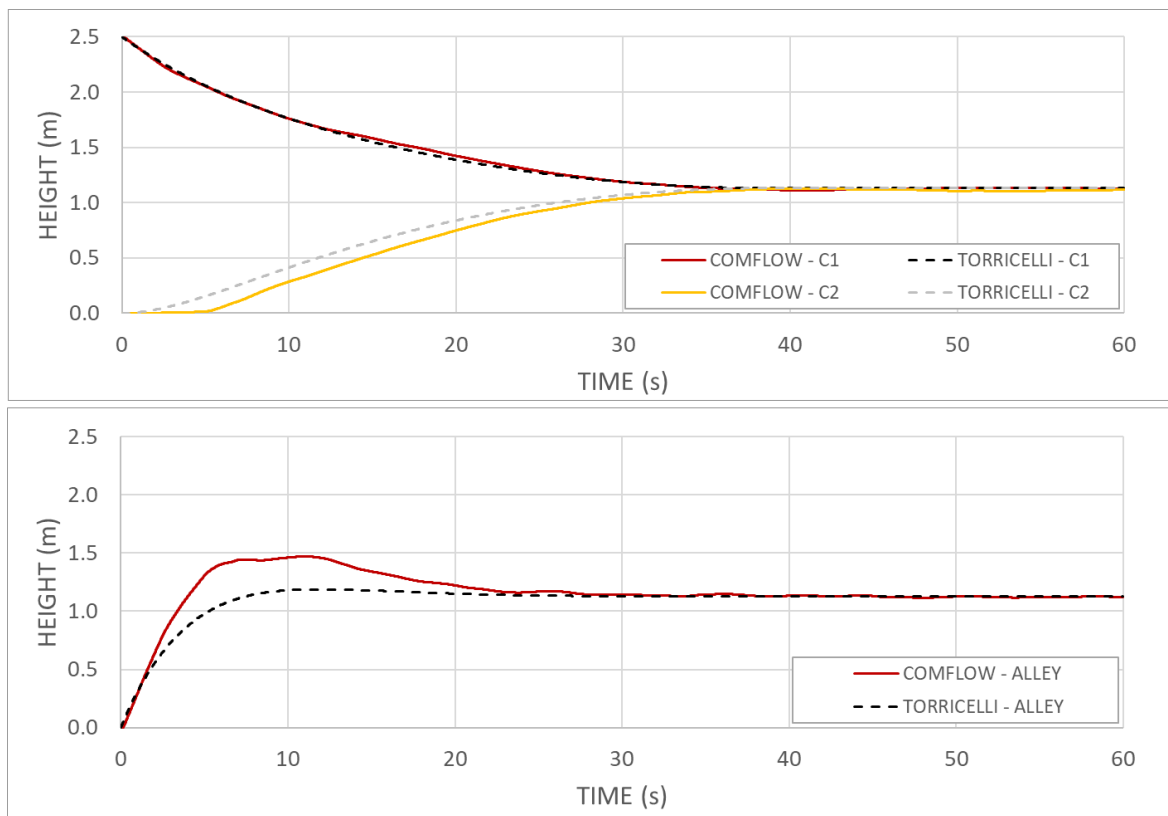


Figure 4-6: The time trace comparison of the mean filling level in each compartment from COMFLOW and from a hydraulic model (MARIN-UIF) using the Torricelli law. The default discharge coefficient of 0.6 is used. The flow reduction in C1 is very well predicted. the filling rate of C2 is somewhat different, but the overall performance of the simple flooding model is fully satisfactory for this practical case.

### 4.3.3 Compartment modelling / Air entrapment

In the section above air entrapment is already mentioned as an important factor to consider in numerical modelling, as well as in model tests. It is recommended that the model tests are specific on air entrapment, or use fully ventilated spaces for the purpose of proper benchmarking. Most numerical tools have the capability to include air compression / pressure build up.

It is clear for all users of numerical tools that the “real” ship compartmentation is far more complex than could be modelled in a simulation tool or in model tests. To which extent the compartmentation has to represent the real ship to obtain valid comparable results, remains unknown, it remains to the user to define this at the moment.

The FLARE project is the best common research group to establish and propose a common sense modelling, and to prove the findings through benchmarking via numerical simulations and model testing. This can establish a proper level of accuracy in the assessment of ship survivability.

## 4.4 Hull breaches

During WP4 meetings it was discussed what the opening speed of a hull breach should be or could be, and if it matters. Information from full scale damages due to striking are absent (luckily). It is clear that when the striking and stroke ship are not detached from each other immediately after the damage occurred, that they will mutual influence each other. It can be expected that a large heel towards the damage does not occur at such instance, but only occurs once the two vessels detach. Hence, the consensus is that an instantaneous damage is the most conservative approach in simulations.

Further discussion and some useful derivations on this matter are presented in annex F. The annex is prepared by HSVA.

## 4.5 Leakage and collapse of non-watertight structures

(Author: Dr. Pekka Ruponen, NAPA)

The watertight compartments of passenger ships are usually further subdivided into smaller rooms with non-watertight decks and bulkheads. Some typical examples are illustrated in Figure 4-7 below. These structures can have a notable effect on the flooding progression, and subsequently also on the stability of the damaged ship. The real flooding sequence can only be calculated with time-domain simulation, where the leakage and collapse of the non-watertight structures is reasonably accounted for.

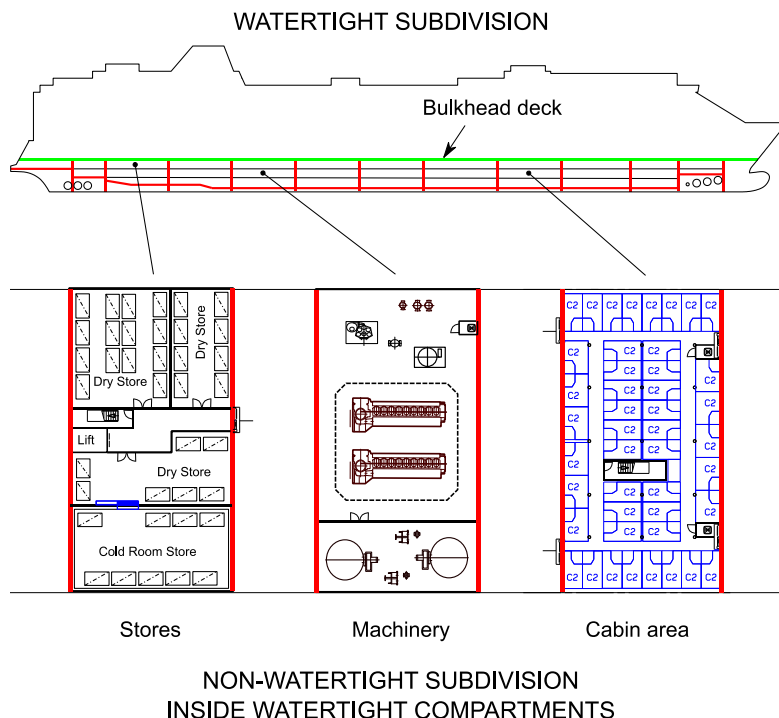


Figure 4-7 Watertight subdivision of a passenger ship with three examples of non-watertight subdivision in some WT compartments, adopted from Jalonen et al. (2017)

Leakage and collapse of non-watertight doors, and their effects on the flooding progression in time-domain, were first discussed by van 't Veer et al. (2004). However, since neither experimental data nor numerical studies were available, educated guesses were used for leakage and collapse parameters of different door types, as presented in SLF47/INF.6. These early studies were motivation for the EU FP7 project FLOODSTAND, where research focused on both full-scale experiments and numerical analyses on leakage and collapse characteristics of various typical non-watertight structures in passenger ship, see Figure 4-8 as adopted from Jakubowski and Bieniek (2010).

A brief summary of the observed leakage and collapse mechanisms for typical non-watertight structures in passenger ships, based on the FLOODSTAND results, is given in annex G.

Moreover, latest research on non-watertight doors in buildings is referenced.



*Figure 4-8 B-class fire rated structures in FLOODSTAND tests, damage to wall around a closed door (left) and significant leaking of a wall (right), photos adopted from Jakubowski and Bieniek (2010)*

#### **4.6 Validation, ITTC Benchmark**

All users have verified and validated their numerical simulation tool through various in-house comparisons, through EU Projects and/or through the participation to the ITTC benchmark studies (2000-2006).

Some validation results are included in the description of the numerical tools in the annexes.

Task WP4.3 report will present the validation against the model tests data from WP4.2.

With reference to Papanikolaou (2007), a brief re-cap is given of the conclusions of the ITTC Benchmark studies. The last benchmark was performed in 2006, almost 15 years ago, so the conclusions might not be fully valid for the status of today's software. Still, the conclusions provide insight in the important aspects that need to be addressed in the simulation tools.

The FLARE benchmark task of WP4.3, open to external FLARE partners as well, will be of great importance and will present a new milestone in the validation of damage stability software.

The ITTC benchmark study results are summarized below:

ITTC Benchmark 1, 2000-2001, main conclusions:

- At present state of knowledge, model tests remain indispensable for assessing the survivability of damaged ships in waves.
- Theoretical-numerical prediction methods can greatly contribute to a pre-assessment of the survivability of intact and damaged ships in waves.

ITTC Benchmark 2, 2004, main conclusions:

- The results from all numerical methods seem to be highly dependent on the viscous roll damping data or the lack thereof.
- The assumed empirical discharge coefficients can have significant outcome on the flooding results, and for tankers in particular, the dynamic flow behaviour of flood water cannot be neglected.

ITTC Benchmark 3, 2006, main conclusions:

- A study of time-to-flood was conducted, showing good correlation between model tests (Ruponen et al 2006) and numerical simulations in steady condition.
- The prediction of flow rates and transient phenomena was less satisfactory.
- As such, reasonable time to sink predictions appear feasible, though with some uncertainty.

## 5 CONCLUSIONS AND RECOMMENDATIONS

### 5.1 Conclusions

All four numerical simulation models are described in sufficient detail with respect to their main modelling assumptions and capabilities. See chapter 3 and the annexes and Volume 2 of this deliverable.

A re-cap is provided of the main numerical aspects, with recommendations for task WP4.2 (model tests) and WP4.3 (benchmarking). This can serve to further improve the numerical model or to verify its assumptions.

All numerical tools rely on user defined discharge coefficients and empirical methods for roll damping (or user input). This contributes to the uncertainty of the outcome of the numerical models. The significance of the user input on the outcome of the simulations is not fully understood, or investigated in all details.

The overall conclusion is that the present state-of-art numerical models can be well applied to achieve the FLARE objectives.

### 5.2 Recommendations

Based on the discussion in chapter 4 in particular, the following is recommended and considered important for the model test task (WP4.2) and benchmark study (WP4.3) thereafter:

- It is crucial to obtain better insight in the viscous roll damping characteristics of a damaged ship in waves. The outcome of the numerical simulations is considered sensitive to the roll damping. The model test data (WP4.2) should provide the basis for the benchmarking (WP4.3).
- Empirical discharge coefficients are an important input for all numerical codes, although the default value of 0.6 seems appropriate on full scale flooding. It is recommended that WP4.2 provides insight in the values that are obtained/valid in the model test experiments (on all typical openings) to avoid the discussion on scale effects.
- It is recommended to study the effect of air entrapment in the model test experiments, and/or to make sure and demonstrate that compartments are fully ventilated. At present there is only limited literature data available on air scaling and on the consequence of entrapment
- It is recommend to measure the wave propagation on large open decks with sufficient accuracy since three out of four numerical models neglect shallow water wave progression. It might be an important feature to improve the flooding models on this point when model tests findings manifest the need for it.



## 6 REFERENCES

- Gao, Z. and Vassalos, D. (2015): The dynamics of the floodwater and the damaged ship in waves, *Journal of Hydrodynamics, Ser. B, Volume 27, Issue 5, October 2015*, pp. 689-695
- Papanikolaou, A. D. (2007): Review of Damage Stability of Ships, Recent Developments and Trends, *Proc. 10<sup>th</sup> Int. Symposium on Practical Design of Ships and Other Floating Structures (PRADS), Houston, October 2007*
- Gao, Z., Gao Q., Vassalos, D. (2011): Numerical Study of Damaged Ship Motion in Waves, *Proc. 12<sup>th</sup> Int. Ship Stability Workshop, Washington D. C., pp. 257-261*
- Gao, Q., and Vassalos, D. (2011): Numerical Study of the Roll Decay of Intact and Damaged Ships, *Proc. 12<sup>th</sup> Int. Ship Stability Workshop, Washington D. C., pp. 277-282*
- De Kat, J.O. and Van 't Veer, R. (2001): Mechanisms and physics leading to the capsize of damaged ships, *Proc. 5<sup>th</sup> Int. Ship Stability Workshop, Trieste, September 2001*
- Ruponen, P. (2007): Progressive flooding of a damaged passenger ship, PhD thesis, Helsinki University of Technology, Department of Mechanical Engineering, November 2007.
- Van 't Veer, R., Peters, W., Rimpelä, A-L., de Kat, J. 2004: Exploring the Influence of Different Arrangements of Semi-Watertight Spaces on Survivability of a Damaged Large Passenger Ship,
- Ruponen, P. 2017: On the effects of non-watertight doors on progressive flooding in a damaged passenger ship, *Ocean Engineering, Vol. 130, pp. 115-125.*
- Jakubowski, P., Bieniek, N. 2010: Experiments with leaking and collapsing structures. FLOODSTAND Deliverable D2.1b. Other report identifications: CTO S.A. RK, No. RK-2010/T-052 /E, CTO reference: 5.167.01.221.
- SLF47/INF.6 2004. Large Passenger Ship Safety: Survivability Investigation of Large Passenger Ships, submitted by Finland, 11th June 2004.
- Idel'chik, I. E. (1960): *Handbook of Hydraulic Resistance* (translated from Russian), Published for the U.S. Atomic Energy Commission, Washington D.C.
- Van 't Veer, R., Serra, A. (2003): Large Passenger Ship Safety: Time to Sink simulations, RINA Conference of Passenger Ship Safety, London, 2003
- Bos, M.G. (1989): *Discharge measurement structures*, Third revised edition, International Institute for Land Reclamation and Improvements/ILRI, Wageningen

## 7 ANNEXES

### 7.1 Annex A: Public summary

Within the FLARE consortium there are four participants that will execute numerical simulations on a damaged Cruise Ship and damaged RoPAX vessel as to benchmark their numerical simulation tool. These numerical simulation tools have been developed over the past years, and most of them have been applied in other EU funded research projects, ITTC benchmark studies or accident investigations (such as the MV Estonia).

From the past experiences knowledge and experience has been gained on how to perform these rather complex simulations that involve large amplitude ship motions in irregular waves in combination with transient and progressive flooding through a complex network of ship compartments. The nature of the problem is highly non-linear and the more complex the ship internal is modelled the more time consuming the whole analysis is. As well, the complexity of the compartmentation does not allow a one-to-one modelling of the real ship internal space in all its details. One has to simplify the internal compartmentation to obtain feasible numerical models. The challenge is to do this while respecting the main flow behaviour during both transient and progressive flooding.

To accommodate the benchmarking of the present state-of-art numerical simulation tools, model tests will be conducted within the FLARE project using various degree of internal representation, with focus on the issue of air entrapment and the scaling thereof, and with focus to the ship hydrodynamics when the vessel is subject to large heel angles that can slowly increase over time as progressive flooding takes on. This will lead to conclusions on the performance of the present tools and recommendation on improvements if needed so that future application of numerical tools lead to a reliable prediction of the ship survivability.

Name of responsible partner: MARIN

Name of responsible person: Riaan van 't Veer

Contact info (e-mail address etc.): Riaan.vantveer@marin.nl

## 7.2 Annex B: PROTEUS3 software

(Author: Alistair Murphy & Luis Guarin (Brookes Bell), prof. Dracos Vassalos (MSRC))

### Software overview

With twenty years of continuous collaborative research and development Brookes Bell Group's software solution PROTEUS3 is capable of modelling in time-domain the dynamic behaviour of intact and damaged vessels in waves and has been validated against numerous model experiments and benchmark tests on various vessel types.

Overviews of its main features and applications are given below. Details of the underlying numerical model, of the requirements of the vessel model and of the application of PROTEUS3 within the FLARE project, are provided in subsequent sections.

### PROTEUS3 Overview



#### Background

- ▶ With over twenty years of continuous collaborative research and development in the field, Brookes Bell Group is one of the market leaders in numerical flooding simulations.
- ▶ The group's in-house developed software solution PROTEUS3 is capable of modelling in time-domain the dynamic behaviour of intact and damaged vessels in waves, and has been validated against numerous model experiments and benchmark tests on various vessel types.



## PROTEUS3 Features



### Summary of main features

- ▶ The feature set of the software has been continuously developed and enhanced to allow for modelling of various types of vessels and internal geometry, and for use in a number of different applications.
- ▶ The software comprises:
  - Advanced calculation engine featuring a time domain solver for 6 DoF ship motions in regular and irregular waves, coupled with empirical and semi-empirical models for calibrated accuracy of predictions.
  - Multi-free surface engine able to accommodate detailed models of internal watertight architecture.
  - Realistic modelling of openings capturing multidirectional collapse heads and variable leak rate flows.
  - Individual control for opening activation/closing times.
  - Ability to apply multiple external moments during the simulation to consider aspects such as wind loading.
  - Detailed motion characteristics for specific user-defined points on a geometric model.
  - Integrated Monte-Carlo sampling algorithm for random generation of collision and grounding damages.



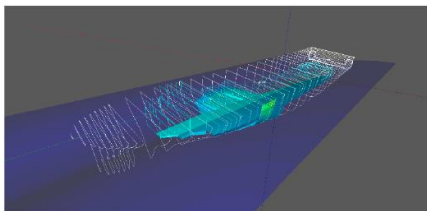
Internal Door leaking tests taken from FLOODSTAND project report

## PROTEUS3 Applications



### Summary of main applications

- ▶ The PROTEUS3 software has been used extensively in the prediction of vessel motions and survival boundaries for estimating the outcome of STOCKHOLM Agreement model tests.
- ▶ The introduction of probabilistic damage stability requirements known as SOLAS'2009 opened up a new market for the software allowing for direct performance assessment based on Monte-Carlo simulations. These simulations provide an overall level of survivability for a vessel, which has been shown to represent a more realistic assessment than that currently obtained from the statutory SOLAS'2009 damage stability calculations. The detailed results from this type of study can be used to highlight areas of low survivability in a design and/or critical openings which lead to progressive flooding and capsize, and potentially can be used to make changes to the vessels' layout to improve these areas. MONTE CARLO simulations have been carried out for several clients on vessel types ranging from Ferries to Cruise Liners.

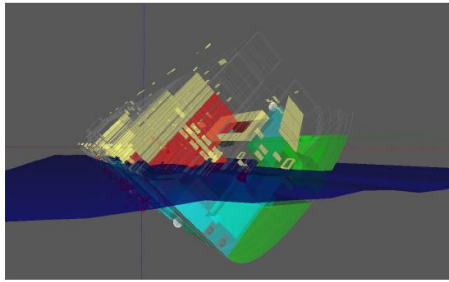


Prediction of STOCKHOLM Agreement model experiments



### Summary of main applications

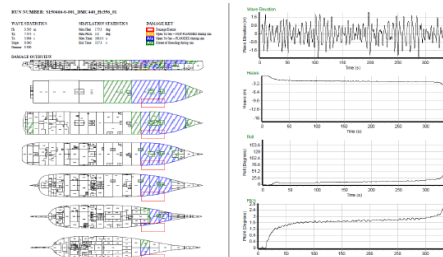
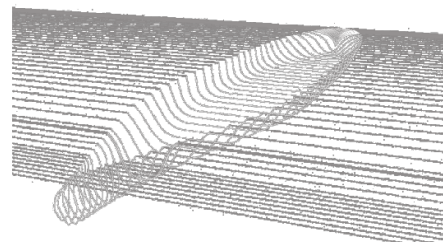
- ▶ An important domain of application is the calculation of ship dynamic responses in relation to comfort analysis in a seaway.
- ▶ The advanced flooding engine and the ability of the software to model the behaviour of a vessel in waves resulted in PROTEUS3 being applied in several high-profile casualty investigations to aid in understanding the sequence of events and the detailed causation of a given incident.
- ▶ Applicable for vessel types ranging from small fishing vessels, cruise liners and large cargo vessels



Forensic reconstruction of vessel incidents

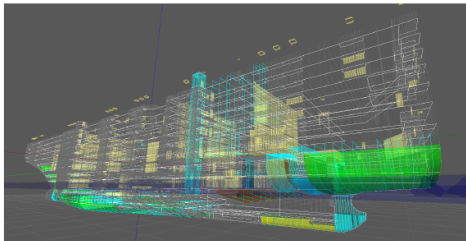
### Engine specifics

- ▶ 6 DoF motions
- ▶ Restoring forces and moments calculated at each time step.
- ▶ Wave forces calculated by means of 2D strip theory and Rankine-source, or 3D Green function method; these include radiation (added mass and damping), diffraction and incident-waves (Froude-Krylov) forces
- ▶ Higher order effects (i.e. drift and current forces) based on parametric, semi-empirical models
- ▶ To account for the large amplitude motions the restoring and Froude-Krylov forces are calculated by direct integration of the water pressure up to the instantaneous wave elevation
- ▶ Viscous forces correction based on the modified Ikeda's method
- ▶ Water ingress/egress based on Bernoulli's equation with empirical discharge coefficient; effects of air compressibility are not taken into consideration (i.e. assumption of perfectly ventilated compartments)
- ▶ Floodwater modelled either by simple model with flat, horizontal free-surface or as free-mass in potential-surface



### Interfaces

- ▶ The geometric model for use in PROTEUS3 can easily be exported from industry standard software packages such as NAPA.
- ▶ Initial condition, loading condition, openings and geometric connection information can be directly imported from external packages such as NAPA and used in the PROTEUS3 model.



Complete complex model geometry exported from NAPA

### Tools

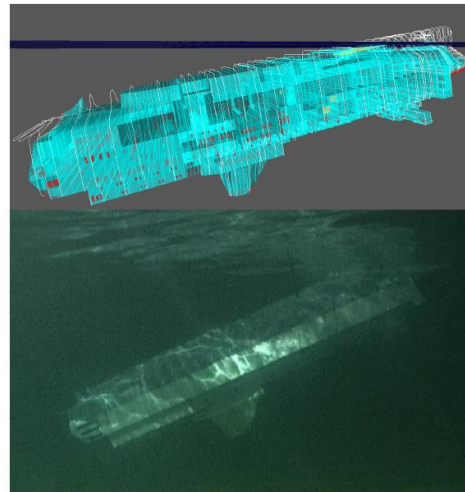
- ▶ Standalone modelling software designed for use with PROTEUS3 allow for fast modelling of openings on large complex vessels such as cruise liners.
- ▶ Standalone batch running and management software allows for large numbers of simulations to be carried out simultaneously in multi-core environments.
- ▶ Standalone 3D viewing software allows simulations to be analysed in detail visualising flow rates, flooding progression, and vessel motions.
- ▶ Standalone reporting software allows for collation of results in graphical and numerical format into PDF files.



Standalone Opening modelling tool

### Track record

- ▶ The PROTEUS3 software has been developed under the companies ISO:9001 quality standard and procedures.
- ▶ Considerable experience has been gained from numerous model experiments carried out on various vessel types. This experience has allowed Brookes Bell to understand the impact various aspects of the modelling have on any given outcome, and allows for internal best practices to be developed when applying numerical simulations to a given problem.
- ▶ The PROTEUS3 tool has itself been tested against real life scenarios when it has been used to reconstruct vessel flooding incidents such as the COSTA CONCORDIA and the MV ESTONIA.
- ▶ The extensive application of PROTEUS3 in the STOCKHOLM Agreement model testing process has provided considerable reference material, which Brookes Bell has used to further refine the software.
- ▶ In addition to the various model experiments carried out, PROTEUS3 was one of the numerical tools tested in several ITTC benchmark studies, namely
  - ITTC Benchmark study for intact stability (reported in 2002)
  - ITTC Benchmark study for damaged ship stability (reported in 2002)
  - ITTC Benchmark on Numerical Prediction of Damage Ship Stability (reported 2004, 2008)
  - ITTC Benchmark Study on Numerical Codes for the Prediction of Time to Flood of Ships (reported 2008)



PROTEUS simulating the sinking of the model of the MV ESTONIA

### Research Projects

- ▶ 1999 – 2002 Harmonisation of Probabilistic Rules and Design Rationale - HARDER
- ▶ 1999 – 2002 Probabilistic Rules-based Optimal Design of Ro-Ro Passenger Ships – ROROPROB
- ▶ 1999 – 2002 First Principles Design for Damage Resistance against Capsize – NEREUS
- ▶ 2001 – 2005 An Integrated Approach to Safe European Ro-Ro Ferry Design – SAFER EURORO II
- ▶ 2002 – 2003 Time Based Survival Criteria for Passenger Ro-Ro Vessels (MCA)
- ▶ GOALDS (Goal-based Damage Stability)
- ▶ 2002 – 2006 Safe and environmentally friendly passenger ships SAFENVSHIP
- ▶ 2003 – 2005 Integrated Crisis and Operation Management Decision Support System for Passenger Ships (COMAND)
- ▶ 2004 – 2007 Safe Abandoning of Ships (SAFECRAFTS)
- ▶ 2007 RP564 Investigation into the safety of ro-ro passenger ships fitted with long lower holds 1 (MCA)
- ▶ 2007 – 2009 RP592 Investigation into the safety of ro-ro passenger ships fitted with long lower holds 2 (MCA)
- ▶ 2007 – 2010 EU Framework for Safe, Efficient and Environmentally-Friendly Ship Operations (FLAGSHIP)
- ▶ 2005 – 2009 Design/Operation/Regulation (IP – SAFEDOR)
- ▶ 2009 – 2012 Standards for Casualty Mitigation, Damage Stability and Subdivision (FLOODSTAND)
- ▶ 2009 – 2012 Goal-Based Damage Stability (GOALDS)
- ▶ 2010 – 2011 Study of the specific damage stability parameters of Ro-Ro passenger vessels according to SOLAS'2009, including water on deck calculation (VINOVA Sweden)

### Commercial Projects

- ▶ Used on 100+ projects for estimating the likely outcome of STOCKHOLM Agreement model experiments
- ▶ Flooding simulations on the COSTA CONCORDIA accident
- ▶ MV Estonia Forensic Study
- ▶ Survivability assessment of RCCL new buildings (from GENESIS class to EDGE project)
- ▶ Survivability assessment of special purpose ships (rock installation vessels) in support of design risk analysis (for ULSTEIN Design)

### Summary of main features

The feature set of the software is being continuously developed and enhanced to allow for modelling of various types of vessels and internal geometries, and for use in a number of different applications. The software comprises:

- Advanced calculation engine featuring a time domain solver for 6 DoF ship motions in regular and irregular waves, coupled with empirical and semi-empirical models for calibrated accuracy of predictions.
- Multi-free surface engine able to accommodate detailed models of internal watertight architecture.
- Realistic modelling of openings capturing multidirectional collapse heads and variable leak rate flows.
- Individual control for opening activation/closing times.
- Ability to apply multiple external moments during the simulation to consider aspects such as wind loading.
- Detailed motion characteristics for specific user-defined points on a geometric model.
- Integrated Monte-Carlo sampling algorithm for random generation of collision and grounding damages.

## Summary of main applications

- The PROTEUS3 software has been used extensively in the prediction of vessel motions and survival boundaries for estimating the outcome of STOCKHOLM Agreement model tests.
- The introduction of statutory probabilistic damage stability requirements (SOLAS'2009), combined with the evolution of the cruise ship market, lead to a market demand for new and innovative solutions for assessing the safety level of such large vessels. In response Brookes Bell Group developed and enhanced the software to allow direct safety level assessment based on Monte-Carlo simulations. These simulations provide an overall level of survivability for a vessel, which has been shown to represent a more realistic assessment than that currently obtained from the statutory damage stability calculations. The detailed results from this type of study can be used to highlight areas of low survivability in a design and/or critical openings which lead to progressive flooding and capsizing. This knowledge can be used to make improvements to a vessel's arrangement where required. MONTE CARLO simulations have been carried out for several clients on vessel types ranging from Ferries to Cruise Liners.
- An important domain of application is the calculation of ship dynamic responses in relation to comfort analysis in a seaway.
- The advanced flooding engine and the ability of the software to model the behaviour of a vessel in waves resulted in PROTEUS3 being applied in several high-profile casualty investigations to aid in understanding the sequence of events and the detailed causation of a given incident.
- Applicable for vessel types ranging from small fishing vessels, cruise liners and large cargo vessels

## Numerical model

A summary of the of the underlying Numerical Model is given below. A detailed description can be found in reference [1].

### Ship Dynamics

- 6 Degree-of-Freedom motions derived from rigid-body theory.
- The effects of floodwater dynamics are included.

### Ship Hydrodynamics

- Ship hydrodynamics, derived from properties of the intact hull, are based on asymmetrical strip theory formulation with Rankine source distribution accounting for non-linearities arising from instantaneous variation of the mean ship attitude and large amplitude motions.

### Internal Effects

- Floodwater motions are modelled as a Free-Mass-on-Potential-Surface (FMPS) decoupled system in an acceleration field.



- Water ingress/egress is based on Bernoulli's equation, with an associated flow loss coefficient of 0.6, derived from experimental studies.

### Vessel model

#### Geometry

- Both the hull and compartments comprising the internal arrangement are accurately and efficiently defined by calculation sections, reducing the calculation overhead imposed by geometric calculations.
- While shell thickness is handled directly in the definition of the hull, individual compartments each have an associated permeability.

#### Compartment Connections and Openings

Individual compartments can be connected in one of two ways:

- Via "Compartment Connections" such that they are handled as a single geometric object. Multiple compartments can be connected in this manner.
- Via specific openings (e.g. representing a hinged door, or a bulkhead opening) defined by the following parameters:
  - Location, dimensions and orientation
  - Connected compartments
  - Collapse pressures and leakage rates. See reference [2].
  - Separate collapse pressures and leakage rates can be defined for each side of the opening (e.g. to handle the opening direction of a hinged door when it experiences flooding on only one side).

#### Loading Condition

- The vessel can be loaded via both point masses and fluid loads.
- A fluid load of a specified density is associated with an individual compartment.



## Application within FLARE

### WP4 – Numerical Simulations and Verification

- Task 4.3: Benchmarking and Verification

### WP5 – Flooding Risk Model

- Task 5.2.2: Dynamic Vulnerability Screening
- Task 5.2.3: Forensic Examination of Critical Scenarios

## References

[1] Jasionowski, A, 2001. *An Integrated Approach to Damage Ship Survivability Assessment [dissertation]*. [GLASGOW UK]: University of Strathclyde.

[2] FLOODSTAND (2009-2012) *Guidelines and Criteria On Leakage Occurrence Modelling*. European Commission, Seventh Framework Programme (FP7), Project Reference: FP7-RTD-218532. Available at: [http://floodstand.aalto.fi/Info/Files/Floodstand\\_D2.2b\\_final\\_20110225.pdf](http://floodstand.aalto.fi/Info/Files/Floodstand_D2.2b_final_20110225.pdf)



## 7.3 Annex C: NAPA flooding software

(Author: Dr. Pekka Ruponen (NAPA))

### Introduction

NAPA Flooding Simulation tool is part of the NAPA software package. In principle, it is an alternative option for calculation of a damage case. This is a separately licensed feature in addition to the standard damage stability calculation licence.

The tool is developed for accurate simulation of progressive flooding in complex internal arrangements, typical for passenger ships. The main assumptions and features are listed below:

- Floodwater surface in each flooded room is flat and parallel to the sea level
- Flow through openings is governed by Bernoulli's equation and flow losses are represented by a constant discharge coefficient (user input value, separately for each opening)
- Leakage and collapse of non-watertight structures (e.g. A-class fire doors) can be modelled. Values are user input, and e.g. the FLOODSTAND recommendations can be used
- Air compression and airflows can be calculated for selected compartments (perfect gas & Bernoulli for compressible fluid)
- Ship motions are considered either quasi static or alternatively dynamic roll angle (linear roll damping) with quasi static draft and trim
- Righting lever (GZ) curve can be calculated for each time step with quasi static ship motions
- Waves are excluded in calculation of damaged ship motions, but it is possible to calculate the "wave pumping" effect on in-flooding rate, e.g. to estimate accumulation of water on deck

There is a graphical user interface (GUI), MGR\*FLOODING\_SIMULATION, with dedicated tools for efficient modelling of the openings. NAPA Flooding Simulation is an alternative option to calculate a damage case. Therefore, it is easy to create scripts (NAPA macros) or simple user interfaces for calculation of large number of cases. Monte Carlo simulation can be used for generating the breach extents. Such a study for using simulation to assess survivability level was reported in detail in Ruponen et al. (2019).

Detailed description of the applied method is given in Ruponen (2006, 2007 & 2014). The following sections give an overview of the applied numerical methods and assumptions.

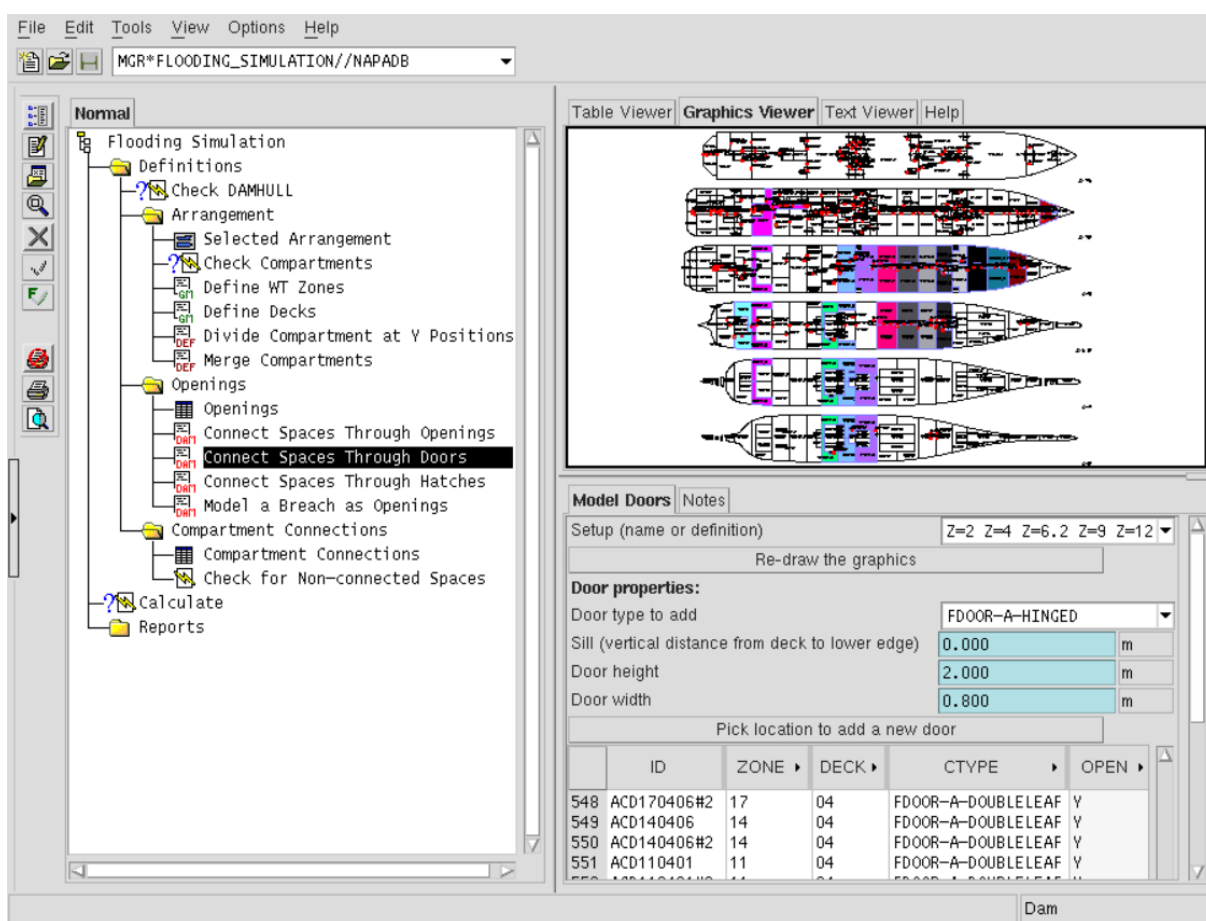


Figure 7-1: MGR\*FLOODING\_SIMULATION, the graphical user interface for NAPA Flooding Simulation, including definitions and calculations

## Governing equations

The applied approach is very similar to grid-based CFD methods. The ship is treated as a *staggered grid*, where each room is one computational cell. These cells are connected to each other through the modelled openings, corresponding the cell faces in the grid.

At each time step, the conservation of mass must be satisfied in each flooded room. The equation of continuity is:

$$\int_{\Omega} \frac{\partial \rho}{\partial t} d\Omega = - \int_{S} \rho \mathbf{v} \cdot d\mathbf{S}$$

Where  $\rho$  is density,  $\mathbf{v}$  is the velocity vector and  $\mathbf{S}$  is the surface that bounds the control volume  $\Omega$ , i.e. the flooded room. The normal vector of the surface points outwards from the control volume.

The velocities in the openings are calculated by applying Bernoulli's equation for a streamline from point A that is in the middle of a flooded room to point B in the opening, see Figure 7-2:

$$\int_A^B \frac{dp}{\rho} + \frac{1}{2}(u_B^2 - u_A^2) + g(h_B - h_A) + \frac{1}{2}k_L u_B^2 = 0$$

Where  $p$  is air pressure,  $u$  is flow velocity and  $h$  is water level height from a common reference level. All losses in the opening are represented by a non-dimensional pressure loss coefficient  $k_L$ . The so-called discharge coefficient for the flow through the opening is related to the pressure-loss coefficient:

$$C_d = \frac{1}{\sqrt{1 + k_L}}$$

Consequently, by denoting the water pressure head by  $H = h_B - h_A$ , and by assuming constant air pressure and  $u_A \approx 0$ , the well-known equation for volumetric flow through small opening with area  $dS$  is obtained:

$$dQ = C_d \sqrt{2gH} dS$$

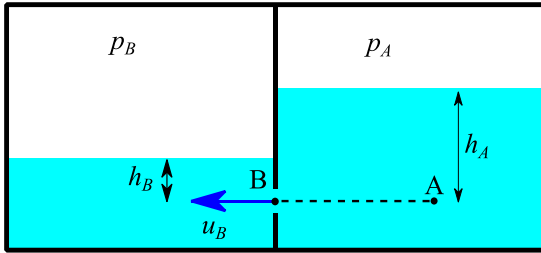


Figure 7-2: Application of Bernoulli's equation for a streamline from point A to point B

### Time discretization

In the simulation algorithm, the instantaneous free surface area  $S_{fs}$  is assumed to be constant within the time step, and therefore, the time derivative of the volume of water in a flooded room  $V_w$  can be presented as:

$$\frac{dV_w}{dt} \approx S_{fs} \frac{dH_w}{dt}$$

Where  $H_w$  is the water level height, measured from the common reference level.

The permeability of the flooded room  $\mu$  is taken into account, so that the effective free surface area is:

$$S_{fs} = \mu S_{tot}$$

Where  $S_{tot}$  is the total area of the cross-section of the room at the floodwater level.

Normally the time derivatives for the pressure-correction algorithm are calculated by using the *three level implicit method*:

$$\dot{H}_w \approx \frac{3H_w^{n+1} - 4H_w^n + H_w^{n-1}}{2\delta t}$$

Where  $\delta t$  is the applied time step.

However, at the steps, where there is potential discontinuity in the flooding rate, the implicit Euler method needs to be used:

$$\dot{H}_w \approx \frac{H_w^{n+1} - H_w^n}{\delta t}$$

A constant time step is used by default, but there is also a calculation option (ADT) that triggers the use of adaptive time step. In this case the user gives the default time step  $\delta t$ , and this is automatically adjusted between  $0.5\delta t$  and  $2\delta t$  based on the changes in the flooding progression and floating position. The details of the algorithm are presented in Ruponen (2014).

### Pressure-correction method

NAPA Flooding Simulation is based on implicit time integration with a pressure-correction algorithm. This has proven to be an efficient and accurate approach for calculation of extensive progressive flooding to several compartments.

In the pressure-correction method, the simulation within a time step is iterative, based on the linearized Bernoulli's equation. The algorithm iterates the pressures in the flooded rooms until both Bernoulli's equation for each opening and continuity for each room is satisfied with sufficient accuracy. After that, the floating position of the ship is calculated on the basis of the distribution of floodwater in the compartments, accounting the free surface effect on all flooded rooms.

A comprehensive description of the pressure-correction method for flooding calculation (and airflows) is given in Ruponen (2007). When only water flows are calculated (constant air pressure), the pressure-correction equation can be presented in matrix format as:

$$\mathbf{A} \cdot \mathbf{H}'_w = -\Delta\mathbf{m}_w$$

Where  $\mathbf{A}$  is a coefficient matrix, with elements depending on the opening characteristics and water levels.  $\mathbf{H}'_w$  is the unknown vector of water height (hydrostatic pressure) corrections and the vector  $\Delta\mathbf{m}_w$  contains the mass balance in each potentially flooded room (residual of the equation of continuity). The water level heights for the next iteration are obtained by adding the corrections to the previous values:

$$\mathbf{H}_w = \mathbf{H}_w^* + \alpha\mathbf{H}'_w$$

Where  $\alpha$  is so-called under relaxation factor. Based on extensive studies, a suitable default value is  $\alpha = 0.5$ . The pressure-correction iteration has converged when mass balance in each room is practically zero, i.e.  $\Delta\mathbf{m}_w \approx \mathbf{0}$ . NAPA flooding simulation automatically decreases the under-relaxation factor  $\alpha$ , if the iteration is not properly converging.

This system of linear equations is trivial to solve. Obviously, the coefficient matrix  $\mathbf{A}$  is often very large and sparse, especially if the number of flooded rooms is large. Thus, application of a proper sparse matrix storage system will ensure the best possible computational performance. In addition, it should be noted that since the method is iterative, it is not necessary to solve the pressure-corrections with high accuracy. Indeed, iterative methods for solution of a system of linear equations have proven to be superior. The conjugate gradient stabilized method (CGSTAB) has been adopted.

### Initial and boundary conditions

The loading condition of the ship before the damage defines the initial condition for the flooding simulation. In NAPA this can be:

- Actual loading condition, including various liquid loads in the tanks
- Simplified initial condition with given floating position and metacentric height (as in SOLAS Ch. II-1 calculations)

It should be noted that the applied method does not handle mixtures of different liquids but loaded water in damaged tanks is treated similarly to floodwater, and thus for example draining of a swimming pool can be simulated.

Furthermore, it is assumed that the impact from a collision or grounding is not affecting the motions of the damaged ship. Consequently, the flooding starts with the ship floating freely with a damage opening in the hull surface.

The surrounding sea is treated as a ghost cell that sets the boundary condition for flooding. The hydrostatic pressure for sea level is calculated based on the floating position for each time step.

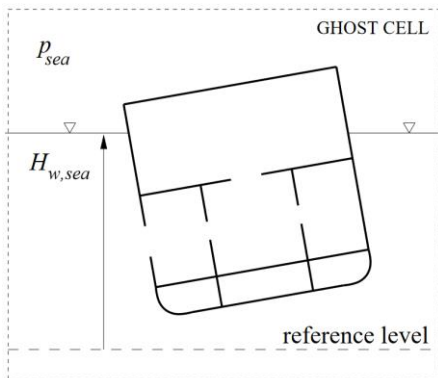


Figure 7-3: Definition of the boundary condition with a ghost cell, Ruponen (2007)

### Calculation of floating position

In NAPA Flooding Simulation, there are two alternative methods for calculation of the floating position at each time step:

- SIM: fully quasi-static (draft, trim and heel in calm water)
- DSIM: dynamic roll angle (with linear damping) combined with quasi static draft and trim in calm water

In fully quasi-static mode, it is also possible to calculate the righting lever (GZ) curve for each time step (or at some interval, e.g. every minute). With DSIM option the natural roll period of the intact ship in and the effective linear roll damping coefficient need to be given as user input (DYNPAR table).

### Simplified method for wave effects on flooding

The ship motions are calculated in calm water with both SIM and DSIM options. However, a simplified method to account for the wave effects on the flooding process has been implemented. This option can be combined with the calculation of dynamic roll motion (see previous section), and all relevant input parameters (wave height, period and spectrum) are given with the option DYNPAR. A beam seas condition with the breach facing the incoming waves is assumed. Currently two wave spectrums (JONSWAP and ITTC) are supported. In addition, regular sinusoidal waves can be used.

The wave elevation, from the calm sea level, can be presented by a sum of the wave components, e.g. Ochi (2005):

$$\zeta(t) = \sum_{j=1}^N a_j \cos(-\omega_j t + \varepsilon_j)$$

In order to ensure that the generated time series does not comprise repeating sequences, a random number generator is used to distribute discrete frequencies ( $\omega_j$ ) and to generate random phase angles ( $\varepsilon_j$ ) of the wave components. The amplitude components ( $a_j$ ) are calculated from the wave spectrum ( $S_\omega$ ):

$$a_j = \sqrt{2S_\omega(\omega_j)\Delta\omega}$$

The pressure head for the damage opening depends on the relative distance between the wave profile and the free surface at the location of the breach opening, Pawlowski (2003). Thus the effective pressure height of the sea that is used as the boundary condition for the progressive flooding calculation is:

$$H_{sea}(t) = H_{sea,calm} + \zeta(t)$$

This sea level height is used to calculate the ingress/egress of water through the breach openings. The approach is simplified, but it is considered applicable to large ships in moderate waves. Most notably, the accumulation of water on the vehicle deck of a RoPax ship can be accounted for.

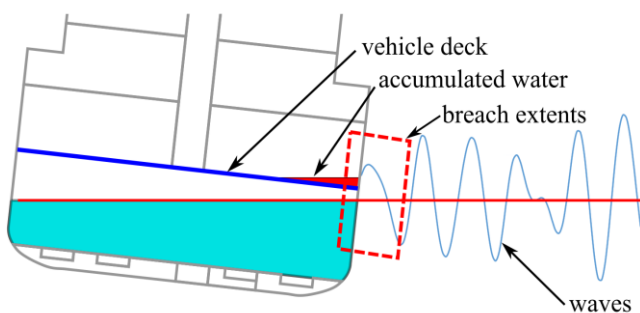


Figure 7-4: Applied model for calculating accumulation of water on deck in simulation

### Modelling principles

Both the rooms in the arrangement and the openings are manually defined by the user. Normal NAPA compartment model used for probabilistic damage calculation often needs to be extended in order to be used with flooding simulation. Details should be added especially

regarding non-watertight subdivision. For this purpose NAPA provides tools for easy modelling in MGR\*FLOODING\_SIMULATION.

## Rooms

Each modelled room is flooded with an individual free surface. Consequently, the so-called “multiple free surfaces” during the flooding process are taken into account. In order to capture the transient asymmetric flooding of symmetrical rooms (e.g. cabin areas), it is necessary to divide these rooms e.g. at centre line and model transverse corridors as openings in this artificial longitudinal bulkhead.

A permeability value is assigned to each modelled room. Normally, this is based on the purpose of the rooms (as defined in the arrangement), but also exceptional values can be given in the range between 0.001 and 1.0.

## Openings

In NAPA each opening connects two rooms. In the case of breaches, the connected room is SEA. In addition to the location (coordinates) and connection, Openings are defined in a table (prefix OPE\*). This definition is tightly coupled with the compartment connection table (CCONN\*). The following parameters should be given:

- AREA: area of the opening (m<sup>2</sup>)
- WRCOEF: discharge coefficient(s) (default is 1.0, but normally 0.6 is used)
- HLEAK: leakage pressure head (default 0.0 m)
- ARATIO: leakage area ratio (default 0.0)
- HCOLL: collapse pressure head (default 0.0 m)
- Status (open/closed), primary definition in the CCONN table OPEN=Y/N

Note that the discharge coefficient is user input. The tool for easy modelling of openings uses a default value of 0.6. There is also support for applying different discharge coefficient for the same opening for the free discharge to air and discharge to water. However, this feature is rarely used.

It is also possible to define the time, when the status of the door is changed (e.g. an initially open WT door is closed). Moreover, the time span for changing the status can be given. During this time span the effective area of the opening is linearly changed. This approach can also be used for breach openings to model the time span that it takes before the full breach is opened.

## Leakage & collapse of non-watertight structures

Leakage and collapse of non-watertight structures under the floodwater pressure are essential for modelling progressive flooding in a passenger ship. An important parameter representing the leakage of a closed non-watertight door/structure is the leakage area ratio:

$$a_{ratio} = \frac{A_{leakage}}{A_{submerged}}$$



Similarly to the critical pressure heads for leakage and collapse, also this parameter is user input in NAPA. The recommendations from the FLOODSTAND project, Jalonen et al. (2017), can be used, unless more accurate data is available.

In NAPA the leakage area ratio can be either a constant value or a function of the effective pressure head  $H_{eff}$ . If only one value is defined, it is used for both directions. When two definitions are given, the applied value depends on the direction of the pressure. The FLOODSTAND recommendations are included, see Figure 7-5, but user can also modify these values, or define new door types with specific leakage and collapse characteristics.

Most notably, the leakage area ratio is irreversible since it is associated with deformation of the door. In practice, this means that  $a_{ratio}$  is evaluated for each (closed) door at every time step. The effective  $a_{ratio}$  value cannot decrease from the previous value, even if  $H_{eff}$  is later decreased.

	OTYPE	HCOLL	HLEAK	ARATIO
1	B-CLASS-JOINER	1.5	0	*0.03* *0.03*HEFF*
2	FDOOR-A-HINGED	2.5	0.0	*0.03*HEFF* *0.02*HEFF*
3	FDOOR-A-SLIDING	1.0	0.0	0.025
4	FDOOR-A-DOUBLELEAF	2.0	0.0	0.025
5	COLDROOM-DOOR	3.5	0.0	*0.01*HEFF*
6	LIFT-DOOR	1.5	0.0	0.03
7	SWT-DOOR	10.0	8.0	0.01

Figure 7-5: Default leakage and collapse parameters for non-watertight doors in modelling for NAPA Flooding Simulation

**Air compression**

Air compression in the flooded compartments can have a notable effect on the flooding progression, especially in tanks and void spaces. In NAPA, all modelled rooms are considered fully vented by default. However, the user can define selected rooms, e.g. tanks and voids, to have restricted ventilation level. In that case, also air pipes should be modelled.

Calculation of air compression is based on the assumption of isothermal process, using the perfect gas law. Consequently, air density as a function of air pressure  $p$  is:

$$\rho(p) = \frac{p}{p_{atm}} \rho_{atm}$$

Where  $\rho_{atm}$  is air density at atmospheric pressure  $p_{atm}$ . In NAPA it is assumed that  $\rho_{atm} = 1.293 \frac{kg}{m^3}$  and  $p_{atm} = 101.325kPa$ . However, it is also possible to give user-defined atmospheric pressure in the reference system.

For airflow calculation, Bernoulli's equation for compressible fluid is applied. Similarly to water flow, the effective discharge coefficient must be defined for all openings and pipes. The applied discharge coefficient for airflow can be different from the discharge coefficient for water flow  $C_{d,air}$ . The volumetric air flow through an opening or pipe with area  $A$ , connecting rooms with air pressures  $p_A$  and  $p_B$  is:

$$Q_{air} = C_{d,air} A \text{sign}(p_A - p_B) \sqrt{2 \frac{p_{atm}}{\rho_{atm}} \left| \ln \left( \frac{p_A}{p_B} \right) \right|}$$

The details of the applied calculation of air compression and airflows are presented in Ruponen et al. (2013), including validation against measurements from full-scale tests with a decommissioned navy vessel.

### Validation studies

NAPA Flooding Simulation tool has been validated with dedicated model tests, using a large-scale model of a box-shaped barge. The results have been extensively reported and analysed in Ruponen (2007) and Ruponen et al. (2007). The experimental results were submitted to the Phase I of the ITTC Benchmark Study. An overview of the benchmark is proved by van Walree and Papanikolaou (2007).

The nominal scale of the box-shaped barge was 1:10, but notable air compression was measured in several studied flooding scenarios. Since Froude scaling law does not apply for air compression, the test results are not scalable to full-scale. Therefore, in order to avoid the scale effects, unique full-scale flooding tests were later carried out with a decommissioned fast attack craft of the Finnish Navy. These tests, along with further validation of NAPA Flooding Simulation have been presented by Ruponen et al. (2010), and a more extensive analysis, focussing on air compression effects, is given in Ruponen et al. (2013). Some examples of the previous validation results are shown in Figure 7-6 and Figure 7-7.

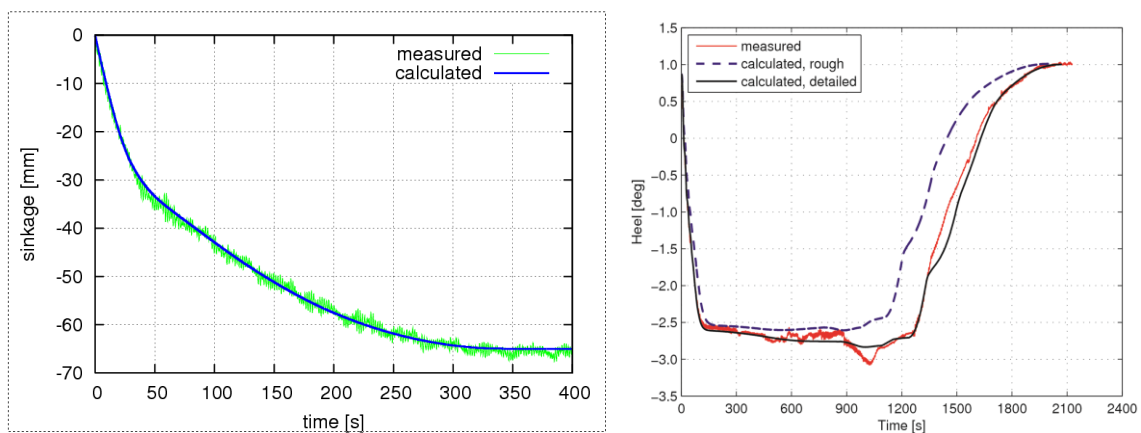


Figure 7-6: Examples of previous validation results from Ruponen et al. (2007 & 2010)

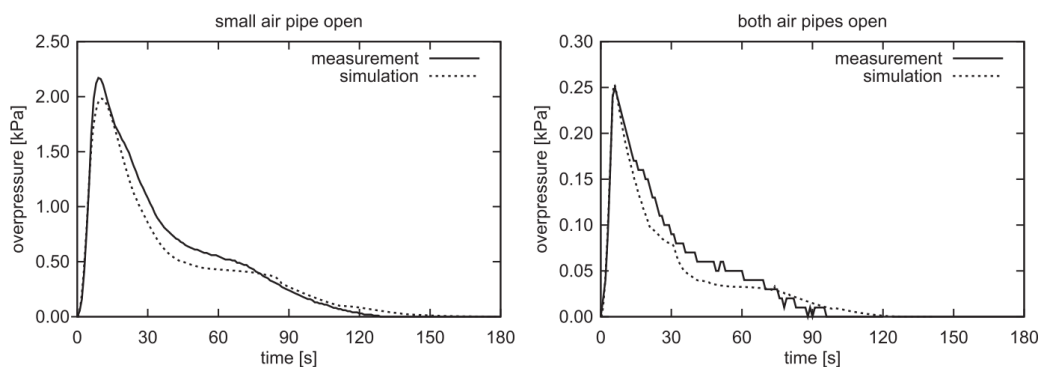


Figure 7-7: Validation results for air compression in a full-scale flooded tank, Ruponen et al. (2013)

## References

- Jalonen, R., Ruponen, P., Weryk, M., Naar, H. and Vaher, S. 2017. A study on leakage and collapse of non-watertight ship doors under floodwater pressure, *Marine Structures*, Vol. 51, pp. 188-201. <http://dx.doi.org/10.1016/j.marstruc.2016.10.010>
- Ochi, M. 2005. *Ocean Waves – The Stochastic Approach*, Cambridge University Press, 319 p.
- Pawlowski, M. 2003. Accumulation of Water on the Vehicle Deck, *Proc. Instn Mech. Engrs Vol. 217 Part M: J. Engineering for the Maritime Environment*, pp.201-211. <http://dx.doi.org/10.1177/147509020321700403>
- Ruponen, P. 2006. Pressure-Correction Method for Simulation of Progressive Flooding and Internal Airflows, *Ship Technology Research – Schiffstechnik*, Vol. 53, pp. 63-73.
- Ruponen, P. 2007. *Progressive Flooding of a Damaged Passenger Ship*, Dissertation for the degree of Doctor of Science in Technology, TKK Dissertations 94, 124 p.
- Ruponen, P., Sundell, T., Larmela, M. 2007. Validation of a simulation method for progressive flooding. *International Shipbuilding Progress*, 54(4), pp. 305–321.
- Ruponen, P., Kurvinen, P., Saisto, I., Harras, J. 2010. Experimental and Numerical Study on Progressive Flooding in Full-Scale, *Transactions of Royal Institute of Naval Architects*, Vol. 152, Part A4, *International Journal of Maritime Engineering*, pp. A-197-207.
- Ruponen, P., Kurvinen, P., Saisto, I., Harras, J. 2013. Air Compression in a Flooded Tank of a Damaged Ship, *Ocean Engineering*, Vol. 57, pp. 64-71. <https://doi.org/10.1016/j.oceaneng.2012.09.014>
- Ruponen, P. 2014. Adaptive time step in simulation of progressive flooding, *Ocean Engineering*, Vol. 78, pp. 35-44. <http://dx.doi.org/10.1016/j.oceaneng.2013.12.014>
- Ruponen, P., Manderbacka, T., Lindroth, D. 2018. On the calculation of the righting lever curve for a damaged ship, *Ocean Engineering*, Vol. 149, pp. 313-324. <https://doi.org/10.1016/j.oceaneng.2017.12.036>
- Ruponen, P., Lindroth, D., Routi, A. L., Aartovaara, M. 2019. Simulation-based analysis method for damage survivability of passenger ships. *Ship Technology Research*, Vol. 66, No. 3, pp. 180-192. <https://doi.org/10.1080/09377255.2019.1598629>
- Van Walree, F., Papanikolaou, A. 2007. Benchmark study of numerical codes for the prediction of time to flood of ships: Phase I, *Proceedings of the 9<sup>th</sup> International Ship Stability Workshop ISSW2007*, Hamburg, Germany.



## 7.4 Annex D: HSVA Rolls software

(Author: Dr. Petri Valanto)

### Introduction

Simulations of non-linear ship roll motions in seaway can be used to predict the frequency of occurrence of excessive roll angles or excessive transverse accelerations, e.g. for purposes of passenger comfort or ship safety. In principle, current numerical field methods for simulating free-surface flows can be used for this purpose. If applied properly, they will give fairly good results for individual cases. However, for deriving reliable frequencies of occurrence for seldom occurring events like capsizing or extreme roll angles in a natural seaway, fairly long time-simulations are needed. These would take more computer and human modelling resources than practical for serious investigations in the industry. See e.g. (Söding et. al., 2013). It is further noteworthy that most field methods dealing with viscous flow contain numerical dissipation, which can lead to inaccuracies particularly in long simulations, in which the numerical errors cumulate.

The method Rolls, on the other hand, was originally developed for investigating the capsizing of the container vessel E.L.M.A. Tres in November 1981 (Söding, 1982). Because of the very limited computer power available at that time compared to that of today, the method had to be fast, but nonetheless accurate enough to give reasonable results. The method was first published by Kröger in 1987 in German language. Only little later the program was extended by Petey (1988a) to deal with ships containing damaged compartments, where sloshing and in- and outflow of water takes place.

The program Rolls has turned out to be a success, so that the program, with various modifications made in the meantime, is applied even now to a variety of cases and problems by users in several institutions. The program Rolls is a blended method and its source code is available for these institutions. This allows modification of the program for specific investigative cases with relative ease, which is a factor certainly contributing to the usefulness of Rolls. Because there is still much interest in the method, Söding et. al. (2013) wrote a brief description of the current state of the method, including validation, however, confining that description only to intact ships.

The present description of the HSVA Rolls is an effort to describe the method more in depth and to include also a description of the methods to model the water flow in inner compartments and on decks programmed and taken into use by Petey (1988). The program Rolls, which is still in active use after more than 35 years from its origin, and which has been recently completely re-programmed for intact ships, should benefit from an adequate documentation. This should also serve as a basis for further developments or for improvements.

## The Origin of the Program Rolls

Numerical simulation of the ship motions in irregular seas together with the time-dependent flow in and out of the damaged compartments and on large deck(s) is often carried out in Germany with the program Rolls. The method was established by Söding (1982) and further developed by Kröger (1987) and Petey (1988a). The simulation is based on combining the method developed by Kröger (1987) for intact ships with the method of Petey (1984,1988a,1988b), which deals with the simulation of fluid flow in ship compartments and on decks.

The ship is considered as a six-degree-of-freedom system traveling at a given mean angle relative to the dominant direction of a stationary seaway. The seaway is simulated as a superposition of a large number of component waves having random frequency, direction and phase angle. The random quantities are computed from a given sea spectrum. During the simulation the chosen mean ship speed and mean wave encounter angle remain constant, whereas the instantaneous ship speed and heading are influenced by the ship motions, which are simulated in all six degrees of freedom.

For the heave, pitch, sway and yaw motions, the method uses response amplitude operators (RAO) determined in the frequency domain with a linear strip method, whereas the roll and surge motions of the ship are determined with time-integration, using nonlinear equations of motion, coupled with the other four degrees of freedom. The ship motion history for the first mentioned motion components in a natural seaway is found by superposition of the reactions in regular waves using the mentioned RAOs. Thus these motion components are treated linearly, including hydrostatic and hydrodynamic forces. Also the wave exciting moment and the roll moment induced by the sway and yaw motions of the ship are determined by response amplitude operators evaluated with the strip method.

For the surge and roll motions, on the other hand, the relatively small hydrodynamic effects are treated primarily to account for their influence on the roll and surge motions, but the nonlinear hydrostatic and Froude-Krylov forces are taken into account carefully. The water pressure in still water or in a wave, not disturbed by the presence of the ship (Froude-Krylov pressure) is a very important contribution. In linear form the FK-pressure is equivalent to the righting-lever curve, including its changes in waves.

The linear treatment of the yaw motion in the present program version has the effect that broaching-to in following waves cannot be simulated by the method Rolls, in spite of its strong coupling to the danger of capsizing. On the other hand, other causes of capsizing, like the dangerous decrease of righting lever on a wave crest, possibly leading to a pure loss of ship stability, parametric roll excitation, or water on deck, are accounted for accurately by the method Rolls. Shifting of cargo, except fluids, due to roll motions is not covered by the present versions of Rolls.

The simulation method for fluid flow in ship compartments and on decks was developed by Söding(1982) and Petey (1988a,b) for the inflow and outflow of water through openings and for water motion in deep water tanks and on decks. Special emphasis in the subsequent Chang's version of the program Rolls is placed on simulating realistically the motion of water on deck. Two different methods of computing the internal water flow are used, depending on the height of the water. The change between these two methods can be made automatically



during the simulation according to the actual situation on the deck or in the compartment in question, if the need arises. See Chang and Blume (1998) and Chang (1999a, 1999b):

1. Fluid motion in deeply filled tanks: In this method the free surface of the liquid is assumed to be an oblique plane, since the greatest natural period of the fluid oscillation is much smaller than the dominant period of the ship motions in most cases. The fluid motion is approximated by that of a point mass concentrated in the centre of gravity of the fluid mass. This point mass can move on a curve described by a vector in ship fixed coordinates. The curve is determined by volumetric calculations before starting the simulation.
2. Motion of a shallow fluid layer in tank or compartment: The flow on decks or large open compartments is modelled with the shallow water equations solved with the Glimm's (1965) method, which is essentially a random choice method. It was later developed into a useful numerical tool by Chorin (1976). Dillingham (1979, 1981) was the first to use it for motion studies of a vessel with water on deck.

In the simulations the time is advanced in small increments. The rate of inflow and outflow of water through any opening is estimated from the difference in the water height inside and outside of the opening at each time step. The openings can be located at the shell of a ship or at internal subdivisions between compartments; they may be intended as openings, or they may be produced by damage, e.g. due to a collision with another ship. The variations in the mass, the centre of gravity and the moment of inertia of the ship due to the inflow and outflow are modelled in the program. The forces and moments due to the interior fluid motion in partly flooded rooms and on the vehicle deck are also determined and added to the other moments due to wave excitation, wind etc.

### Program Version HSVA Rolls

Several versions of the program Rolls, originally developed by Prof. Söding and his students in Hamburg, are used in Germany. For this reason the version used in HSVA for simulation of the motions of damaged ships in waves is called the HSVA Rolls.

The HSVA Rolls version is based on the version Chang (March 1999) used by him for RoPaX capsizing and survivability investigations. Blume and Chang (1998) carried out model tests in HSVA, showing also a very positive correlation between the model tests results and computations with the Chang version of the Rolls program.

Valanto (2002, 2006, 2007, 2008, 2009) and Valanto and Soukup (2016) used the HSVA Rolls for several investigations on passenger ship safety for IMO, investigation on the MV Estonia accident, investigation on the safety parameters of IMO Rules for EMSA, and for an accident investigation of a workboat for the German Federal Agency for Technical Relief (THW). During the course of these research and development projects the HSVA Rolls has been several times slightly updated.

In the Chang version the main program and all subroutines were in one data file. It was possible to compile these and the executable functioned without problems. The program, however, contained features to transfer matrix data between the program parts, which were undoubtedly clever, but absolutely not portable, and not very suitable for serious investigations with the program outside a university. The HSVA Rolls code was distributed in a rational manner to several data files representing different program modules and the portability problems were solved mainly by exact definition of matrix sizes in the main program and subroutines.

In the beginning the HSVA Rolls was used under HP-UNIX operating system on a HP Workstation, and later transferred in 2004 to a newer computer operating under Linux. The Fortran single precision accuracy under the new Linux version was lower, thus having a somewhat lower number of significant digits than that of the Fortran of the older HP-UX. In this phase several comparisons were made between the HSVA Rolls HP-UX- single precision version and the single and double precision versions under Linux. Differences in the simulated survival times of damaged ships in waves were found, and as a result of this comparison work it was decided to continue only with the double precision version of the HSVA Rolls in the future. Due to changes in Fortran compilers and operating system versions the random number generation needed to be changed and some other minor updates needed to be carried out.

One very small, but also a very relevant modification for investigations on damaged ships has been added to the HSVA Rolls: In the original version the effect of the ingress water in tanks and on decks during the simulation was taken into account in the simulation of the roll motion, but not for trim. However, even very small changes in trim, sometimes originated by few larger waves, can cause a long-lasting change in the flow pattern on large open decks and thus influence the survivability of the vessel significantly. In the HSVA version this is taken care of by simply using the longitudinal metacentric height together with the trim moment for evaluating the trim change, which considering the overall small trim angles should be sufficiently accurate.

Output routines of the water motion on the open decks were developed for visualization first with Techplot and later with Paraview. This significantly contributed to value of the accident investigations carried out with the HSVA Rolls (Valanto, 2008, 2016), as it made easier to establish causalities in the accident process and to study the correlation between computed flooding processes and those observed in the corresponding model tests.

During the time span of around 20 years of the existence of the HSVA Rolls the computer capacity has enormously increased. This allows already for some time a fully sufficient resolution of the open spaces or compartments, so that the shallow-water-equations describing the water motions on open spaces can be discretized with a high degree of detail and solved with sufficient accuracy. For example discretizing a deck or another compartment with shallow water with 4000-5000 cells would be usual. Figure 7-8 shows a time frame from the simulations of water gradually increasing on a vehicle deck of a small RoPaX ship. Figure 7-9 shows the transient flooding on the deck of a small work boat leading to a rapid capsizing.

The simulations run fairly fast, even when low filled tanks or compartments requiring the computation of a sloshing motion are included, so that the code can be used for investigations which involve a large number of seaways.



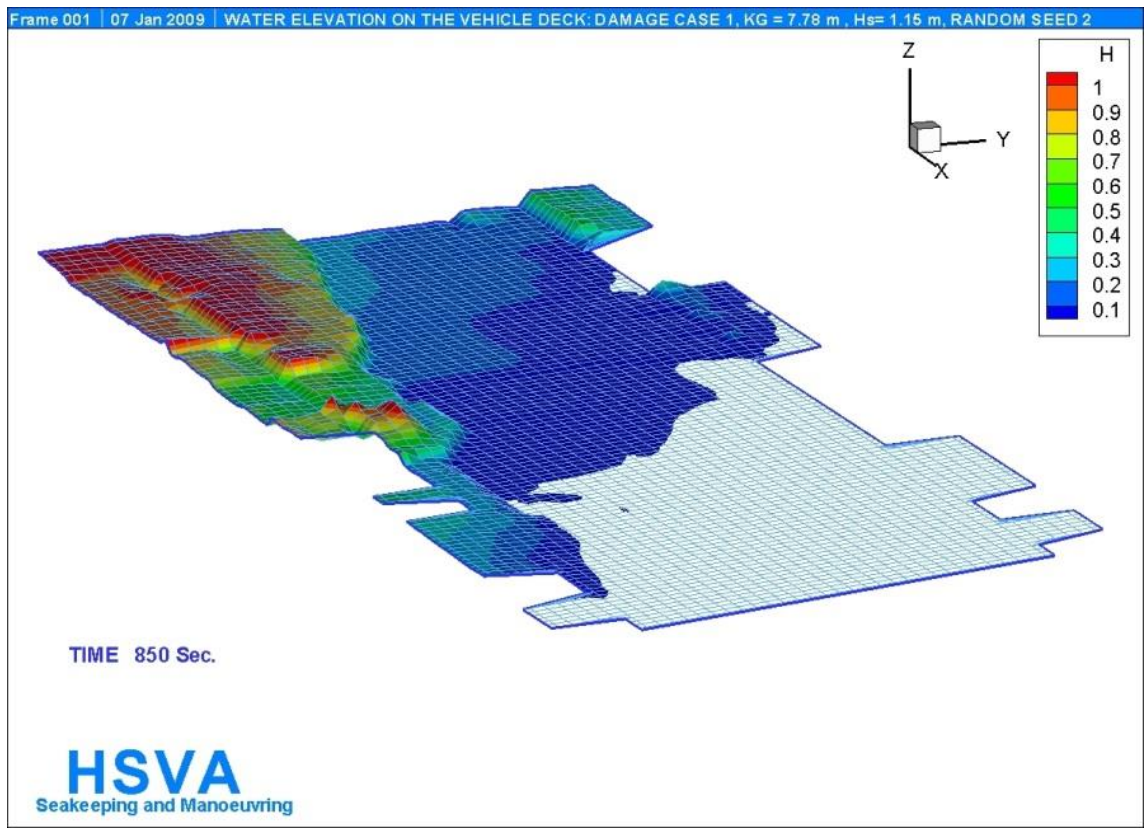


Figure 7-8: Gradual flooding of the vehicle deck of a RoRax ship.

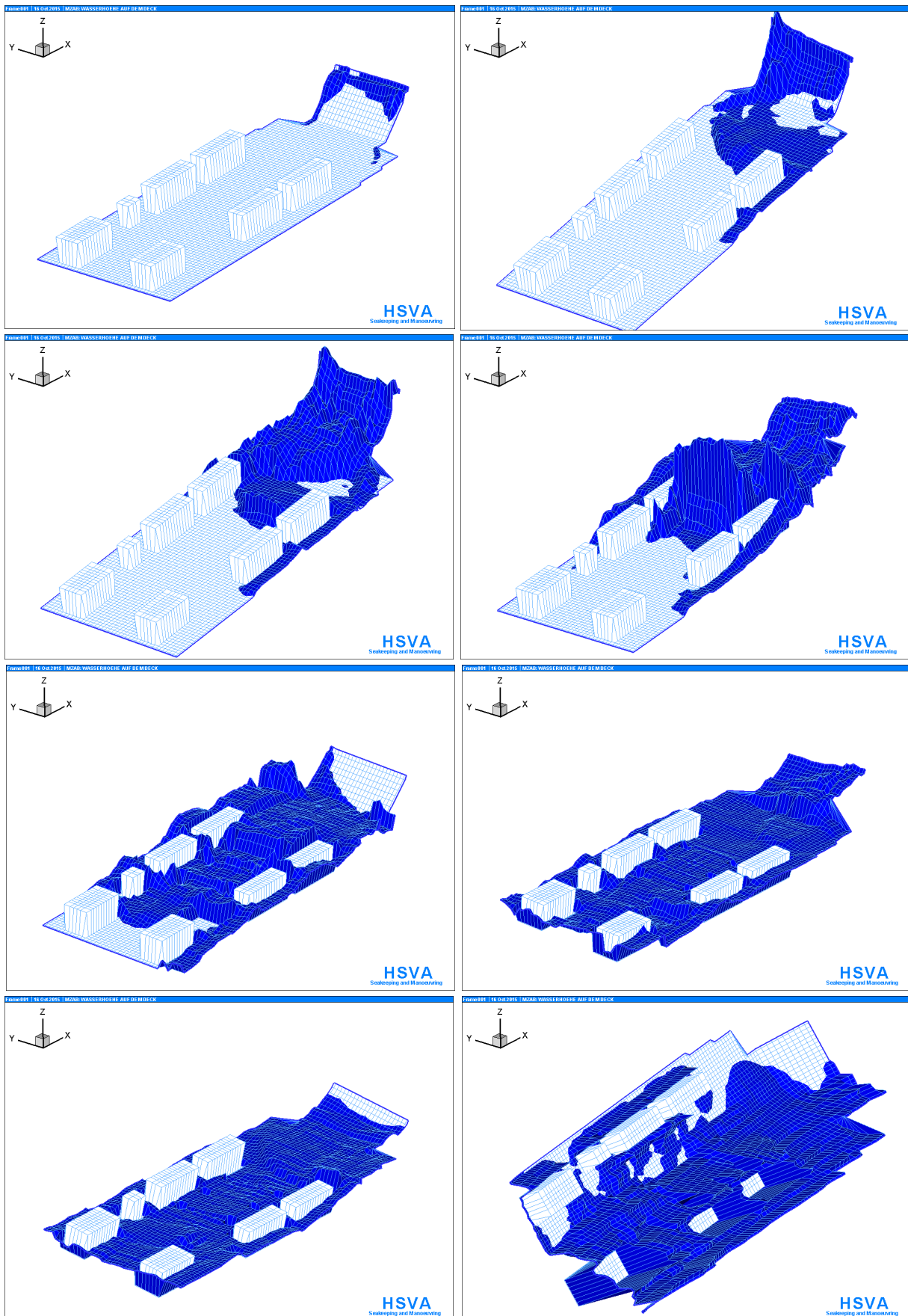


Figure 7-9: Rapid transient flooding of the deck of a work boat: Simulation time, heeling angle and water volume on deck are shown.

## Equation of Roll Motion

### Equations of Motions used in Rolls

The approach in HSVA Rolls to solve the motions of the ship in seaway subject to various external forces is to consider the equations of motions in time domain. Like so many seakeeping codes Rolls is a blended method enabling vital nonlinearities to be captured, while keeping the computational and model preparation time in reasonable size. Both linear and nonlinear force components are incorporated in suitable form. If there is no interaction between certain force components, the method allows them to be added or removed from the equations of motion. This Chapter 3 gives an overview of the theoretical background on how the ship roll motion is treated in (HSVA) Rolls. Chapters 4 to 9 deal with the most relevant modeling details related to this roll motion equation.

The equations of motion related to a ship in confused seas are based on Euler's Laws, which can be expressed as:

- (1) Conservation of linear momentum: The time rate of change of momentum is equal to total forces acting on the body.
- (2) Conservation of angular momentum: The time rate of change of angular momentum is equal to total moments acting on the body.

Euler's laws hold only in an inertial frame of reference. The conservation of linear momentum of the ship can be written

$$\vec{F} = \frac{d\vec{P}}{dt} = \frac{d(m\vec{v})}{dt} = m\ddot{\xi}_G \quad , \quad (1)$$

in which  $\vec{F}$  is the sum of external forces on the ship, and  $\vec{P}$  the linear momentum,  $m$  the body mass,  $\vec{v}$  the velocity vector and  $\ddot{\xi}_G$  the acceleration.

The conservation of angular momentum of the ship can be written

$$\vec{M}_G = \frac{d\vec{H}}{dt} = \frac{d(I_G\vec{\omega})}{dt} = I_G\dot{\vec{\omega}} + \vec{\omega} \times (I_G\vec{\omega}) \quad , \quad (2)$$

in which  $\vec{M}_G$  is the moment of external forces on the ship,  $\vec{H}$  the angular momentum,  $I_G$  the inertia tensor written in matrix form about the center of mass G with respect to  $\xi, \eta, \zeta$  -axes, and  $\vec{\omega}$  is the angular velocity of the ship in the inertial (earth-fixed) coordinate system  $(\xi, \eta, \zeta)$ .

The mass distribution of the ship is best expressed in the ship-fixed coordinate system  $O_{XYZ}$ , in which the moments and products of inertia of the intact ship are time-independent. For this purpose it is necessary to express the matrix of inertia  $I_{G\xi\eta\zeta}$  in terms of inertia moments in ship-fixed coordinates  $(x, y, z)$ , which is done with help of a coordinate transformation matrix.

The elements of this inertia matrix are estimated or determined from the mass distribution of the ship as follows

$$I_{XX} = \int_{\text{all masses}} \left[ (y - y_G)^2 + (z - z_G)^2 \right] dm, \quad I_{XZ} = \int_{\text{all masses}} \left[ (x - x_G)(z - z_G) \right] dm, \quad (3)$$

and correspondingly for the other elements of the inertia matrix, if needed. The integration is performed over all ship masses. If the products of inertia ( $I_{XY}, I_{XZ}, I_{YZ}$ ) in ships are non-zero, these terms constitute an inertial coupling between heel, pitch and yaw motions.

Method Rolls assumes that the ship has a symmetrical mass distribution. Thus the elements  $I_{XY}$  and  $I_{YZ}$  are zero. Inserting the necessary expressions into the conservation of angular momentum (2) and taking only the first  $\xi$ -components gives a relation between the first component  $M_\xi$  of  $\vec{M}_G$  (the roll moment) and roll acceleration. In case of a symmetric mass distribution with respect to y-axis, the following ordinary differential equation for roll motion is obtained:

$$M_\xi = \left[ I_{XX} - I_{XZ} (\psi \sin \varphi + \theta \cos \varphi) \right] \ddot{\varphi} + I_{XZ} \left[ (\ddot{\theta} + \theta \dot{\varphi}^2) \sin \varphi - (\ddot{\psi} + \psi \dot{\varphi}^2) \cos \varphi \right]. \quad (4)$$

Here  $I_{XX}$  and  $I_{XZ}$  are a mass moment and a product of inertia, respectively, referring to the ship center of gravity G in the ship-fixed coordinate system ( $x, y, z$ ). Further  $\varphi$  is the heel angle of the ship,  $\theta$  the trim angle, and  $\psi$  the yaw angle. The derivation of the equation (4) is given in the next chapter in detail.

Other coupling terms between the different motion components are contained in  $M_\xi$ .

$M_\xi$  in (4) is approximated as the sum of several contributions.

## Components of the Heeling Moment in Rolls

### Wave-induced Moments

The water pressure in still water or in an undisturbed wave, that is, not modified by the ship, provides a very important contribution to the righting moment of the ship. It is equivalent to the righting-lever curve, including its changes in waves. Some program versions of Rolls determine this moment due to the water pressure by integrating the pressure over the instantaneous wetted surface, while other versions (like the HSVA version) use stored tables of righting levers computed hydrostatically for a wave-shaped water surface. This latter procedure uses the concept of Grim's equivalent wave (Grim, 1961):

The irregular water surface at any time  $t$  in a natural seaway, which would occur along the center plane of the ship, if this were not present, is approximated within the length range of the ship by an effective wave contour, which approximately produces the same righting ....

## Conclusions

Volume 2 contains a description of the program Rolls and the theory behind it, as used by the HSVA for modelling the behaviour of intact and damaged ships in seaway. The theoretical assumptions behind the program and the linearizations used are described to a high degree of detail. As some formulations used may not appear to the reader as entirely trivial to fathom, also some derivations of the equations used are included. This documentation forms a basis for further development of the program version HSVA Rolls and helps to identify the most relevant topics for the benchmark testing in WP4 Task 4.3.

The origin of the program Rolls lies in the need to have a useful modelling tool for analysing ship flooding accidents. Very much at the first possible opportunity the early developers of the program could take advantage of the at that time very recent advances in modelling shallow-water-equations with the Glimm's method. This gives Rolls a very good capability to model the dynamic or transient water motions on decks. As there is a coupling between the internal fluid motion and the ship motions, the program Rolls is very suitable for modelling both rapid transient flooding cases and cases of slow flooding through water ingress due to wave action leading to gradual capsizing. It is remarkable that no other more recent numerical method so far is able to provide equivalent or better capacity with as small computational and modelling effort.

Experience with the program with suddenly increasing heeling angles resulting in the transition from shallow-water-flow along the deck to accumulation of water at the edge of the deck at high heeling angles works well and gives good results for the purpose of predicting the ship capsizing behaviour. That is, although the limit of validity of the assumption of shallow-water-flow is in some cases clearly violated, the predicted flow and accumulation of water works still very well also beyond this validity limit for the purpose of predicting the heeling behaviour of the ship.

The Glimm's method together with the time-integration leads to water motion which is very similar to that observed in model tests. In more violent cases the numerically predicted water motion can show light to moderate 'random pulsing', which however can make the visual impression of the flow somewhat less attractive. After all there is no viscosity, turbulence or vorticity present smoothing the behaviour of the fully incompressible flow. Visualization is in many cases important and can of course also in case of HSVA Rolls be developed further.

Modelling the flooding of accommodation or public spaces with small compartments or cabins is in general associated with a great difficulty: It is not really possible to model all small geometrical details. On the other hand there are no, at least not yet, suitable models available for describing the delayed or 'seepage' flow through such large compartments consisting of smaller structures being slowly flooded. Once such flow modules become available, they will be of great interest to be included into sea keeping codes dealing with flooding cases.

Ropax ships, however, tend to have such compartments higher up above the large open decks. Thus the flow in such compartments would influence the capsizing behaviour not at all or only at the very late stages in the capsizing process. For classical passenger ships this issue is much more important.

When a damaged ship heels and sinks deeper due to increasing volume and weight of the ingress water, the HSVA Rolls updates the hydrostatics, righting levers, ship mass, ship inertia,

and also the roll damping moment, as this moment is related to the ship displacement and the metacentric height  $GM$ , which are updated at each time-step.

The hydrodynamic RAO's based on computations with the strip method are not updated, but are computed only once for the initial case, most often for the intact case of the ship in upright position. Hennig, et. al. (2006) show a good correlation with tailor-made experiments and Rolls computations also for high roll angles. Brunswig et. al. (2006) compare computations with Rolls to those with the more non-linear code Simbel and also to experiments and show very reasonable results also for the code Rolls. Thus the simplifications in Rolls do not appear to deteriorate the accuracy of the numerical predictions to any significant level.

Any seakeeping code at least partly based on (inviscid) potential theory requires viscous roll damping to be additionally prescribed. For this the program Rolls uses empirical damping coefficients measured in model tests as input to yield good results. Model basins, like HSVA, usually have such data available, either from the ship in question, or from similar ships tested earlier.

There is much less such data available, when the ship heels and the draught increases due to the weight of ingress water in ship. More information on the behaviour of the roll damping coefficients in such a case is desired.

It is known that if the ship hull has a (damage) opening its roll damping coefficients are usually much larger than those for an intact ship of equal displacement. Also the inertia moment of the ship around its roll axis changes, as the hydrodynamic mass of the ship changes due to the damage. This holds also when the water in the ship is not moving and thus causing damping like a roll damping tank, because already the viscous flow around the uneven damage opening tends to cause flow separation and vorticity leading to increased viscous damping.

Thus for the optimal numerical simulation of the ship behaviour in damage cases also the changes in the roll damping coefficients themselves due to increased heel and draught and due to the influence of the damage opening should be taken into account. How significant this is for the accuracy of the numerical modelling can be concluded when more such roll damping data is available.

## References

- Blendermann, W. (1986). Windkräfte am Schiff. Institut für Schiffbau der Universität Hamburg, Bericht Nr. 467.
- Blendermann, W. (1993). Wind forces. In Brix (ed.), *Manoeuvring Technical Manual*, ISBN 3-87743-902-0
- Blendermann, W. (2002). Short-term and long-term statistics of the wind loads on ships. *Ship Technology Research - Schiffstechnik*, 49:160–173
- Blume, P. (1976). Zur Frage der erregenden Längskraft in von achtern kommenden regelmäßigen Wellen. Report No. 334, Institut für Schiffbau Hamburg
- Blume, P. (1979). Experimentelle Bestimmung von Koeffizienten der wirksamen Rolldämpfung und ihre Anwendung zur Abschätzung extremer Rollwinkel. *Ship Technology Research - Schiffstechnik*, 25(1), pp. 3–29
- Böttcher, H. (1986). Ship motion simulation in a seaway using detailed hydrodynamic force coefficients. In 3-rd Int. Conf. on Stability of Ships and Ocean Vehicles, Gdansk
- Brix, J. (1993). *Manoeuvring Technical Manual*. Hamburg, ISBN 3-87743-902-0
- Brunswig, J., Pereira, R. and Kim, D. (2006). Validation of parametric roll motion predictions for a modern containership design. In 9th Int. Conf. on Stability of Ships and Ocean Vehicles, Sao Paolo.
- Chang, B-C. and Blume, P. (1998). Survivability of Damaged Ro-Ro Passenger Vessels, *Ship Technology Research - Schiffstechnik*, 45, pp. 105-117.
- Chang, B-C. (1999a). On the Survivability of Damaged Ro-Ro Vessels Using a Simulation Method. Institut für Schiffbau der Universität Hamburg, Bericht Nr. 597.
- Chang, B-C. (1999b). On the Damage Survivability of Ro-Ro Ships Investigated by Motion Simulation in a Seaway, *Ship Technology Research - Schiffstechnik*, 46, pp. 192–207.
- Chorin, A.J. (1976). Random Choice Solution of Hyperbolic Systems, *Journal of Computational Physics*, Vol. 22, No. 4, Dec. 1976, pp. 517-533.
- Colella, P. (1978). An Analysis of the Effect Operator Splitting and of the Sampling Procedure on the Accuracy of Glimm's Method. Ph.D. Thesis, Lawrence Berkeley Laboratory Report LBL-8774, University of California, Berkeley. 187 p.
- Colella, P. (1982). Glimm's method for gas dynamics, *SIAM Journal on Scientific and Statistical Computing*, 1982 (3) 1, pp. 76-110. 10.1137/0903007. hal-01635216.
- Concus, P., and Proskurowski, W. (1977). Numerical Solution of a Nonlinear Hyperbolic Equation by the Random Choice Method. Lawrence Berkeley Laboratory Report LBL-6487, University of California, Berkeley. 30 p.
- Dillingham, J. (1979). Motion Predictions for a Vessel with Shallow Water on Deck, Ph.D. Dissertation, University of California, Berkeley. 163 p.
- Dillingham, J. (1981). Motion Studies of a Vessel with Water on Deck, *Marine Technology*, Vol. 18 No. 1, 1981.
- Dillingham, J. and Falzarano, J. (1986). Three-Dimensional Numerical Simulation of Green Water on Deck. Third International Conference on Stability of Ships and Ocean Vehicles, Gdansk, Sept. 1986, pp. 57-64.
- Gadd, G. E. (1964). Bilge Keels and Bilge Vanes. National Physical Lab., Ship Division, Report 64.



- Glimm, J. (1965). Solutions in the Large for Nonlinear Hyperbolic Systems of Equations, Communications on Pure and Applied Mathematics, Vol. 18, 1965.
- Grim, O. (1961). Beitrag zu dem Problem der Sicherheit des Schiffes im Seegang. Schiff und Hafen, No. 6.
- Grim, O., and Schenzle, P. (1969). Der Einfluß der Fahrtgeschwindigkeit auf die Torsionsbelastung eines Schiffes im Seegang, Institut für Schiffbau der Universität Hamburg, Bericht Nr. 241.
- Hennig, J., Billerbeck, H., Clauss, G., Testa, D., Brink, K.-E. and Kühnlein, W. L. (2006). Qualitative and quantitative validation of a numerical code for the realistic simulation of various ship motion scenarios. In 25-th Int. Conf. on Offshore Mechanics and Arctic Engineering OMAE 2006, Hamburg, Germany.
- Huang, J., Cong, J., Grochowalski, S., Hsiung, C.C. (1998). Capsize Analysis for Ships with Water Shipping On and Off the Deck. Twenty-Second Symposium on Naval Hydrodynamics, August 9-14, 1998, Washington, D.C.
- Ikedo Y., Himeno Y., Tanaka N. (1978). A Prediction Method for Ship Roll Damping; Report of Department of Naval Architecture; University of Osaka Prefecture, No. 00405.
- JAIC Suppl. No. 504 (1996). Karppinen, T., Rantanen, A., MV Estonia Accident Investigation – Stability calculations, Technical Report VALC177, VTT Manufacturing Technology, Espoo.
- Kirsch. M. (1969). Die Berechnung der Bewegungsgrößen der gekoppelten Tauch- und Stampfbewegungen nach der erweiterten Streifentheorie vom Grim und die Berechnung der Wahrscheinlichkeit für das Überschreiten bestimmter Schranken durch diese Größen, Institut für Schiffbau der Universität Hamburg, Bericht Nr. 241.
- Kröger, P. (1987). Rollsimulation von Schiffen im Seegang, Schiffstechnik 33/4, P. 187-216.
- Krüger, S. (2013). Hydrostatik von Schiffen, [http://www.ssi.tu-harburg.de/doc/webseiten\\_dokumente/ssi/vorlesungsunterlagen/Hydrostatik\\_Skript.pdf](http://www.ssi.tu-harburg.de/doc/webseiten_dokumente/ssi/vorlesungsunterlagen/Hydrostatik_Skript.pdf)
- Ludwig, N. (2006). MV Estonia – Forced Roll damping Tests, HSVA Report S544/06, Hamburg. 28 pp.
- Martin, M. (1958). Roll Damping due to Bilge Keels. Iowa Institute of Hydraulic Research, Report Contr. No. 1611 (01).
- Peltonen, P. (2015). Application of the random choice method to shallow water equations, SCIENCE + TECHNOLOGY 17/2015, Aalto University publication series, Helsinki, Finland, ISBN 978-952-60-6580-9 (pdf).
- Perez, T., Fossen, Th. (2007) Kinematic Models for Manoeuvring and Seakeeping of Marine Vessels, Modeling, Identification and Control, Vol. 28, No. 1, pp. 19–30.
- Petey, F. (1984). Berechnung der Flüssigkeitsbewegungen in teilgefüllten Tanks und Leckräumen. Bericht Nr. 447, Schriftenreihe Schiffbau, Technische Universität Hamburg-Harburg (TUHH), Hamburg.
- Petey, F. (1986). Numerical Calculation of Forces and Moments due to Fluid Motion in Tanks and Damaged Compartments. Proceedings of STAB`86 Conference.
- Petey, F. (1988a). Ermittlung der Kentersicherheit lecker Schiffe im Seegang. Bericht Nr. 487, Institut für Schiffbau, Hamburg.
- Petey, F. (1988b). Ermittlung der Kentersicherheit lecker Schiffe im Seegang. Schiffstechnik 35/4, 155-172.
- Shigunov, V., Moctar, O. E. and Rathje, H. (2009). On conditions of parametric rolling. In 10-th Int. Conf. on Stability of Ships and Ocean Vehicles, St.-Petersburg.
- Söding, H. (1982). Leckstabilität im Seegang. Institut für Schiffbau der Universität Hamburg, Bericht Nr. 429, Hamburg.

- Söding, H. (2002). Simulation of the Motions of Damaged Ships in Waves. DCAMM Ph.D.- course Stability of Ships, Lyngby, Denmark.
- Söding, H., Schigunov, V., Zorn, T., Soukup, P. (2013). Method *rolls* for Simulating Roll Motions of Ships, Ship Technology Research 60(2): p. 70-84, Univ. Duisburg-Essen, Germany.
- Stoker, J.J. (1957). Water Waves, the Mathematical Theory with Applications. Interscience Publishers Inc., New York, 567 p.
- Valanto, P., Time-Dependent Survival Probability of a Damaged Passenger Ship, HSVA Report No. CFD 05/2002 Vol. 1 (Capsizing) für IMO SLF 45 in London 2002.
- Valanto, P., (2006). Time-Dependent Survival Probability of a Damaged Passenger Ship II – Evacuation in Seaway and Capsizing, HSVA Report No. 1661. [www.hsva.de](http://www.hsva.de) (IMO-Document SLF 49 Inf. 5 for IMO SLF 49 in London 2006)
- Valanto, P., (2007). New Research into the MV Estonia Disaster, Proceedings of the 9th International Ship Stability Workshop, Hamburg Germany.
- Valanto, P., (2008). Research Study on the Sinking Sequence and Evacuation of the MV Estonia, HSVA Report No. 1663. [www.hsva.de](http://www.hsva.de)
- Valanto, P., (2009). Research for the Parameters of the Damage Stability Rules including the Calculation of Water on Deck of Ro-Ro-Passenger Vessels, for the amendment of the Directives 2003/25/EC and 98/18/EC, HSVA Report No. 1669. [www.emsa.europa.eu](http://www.emsa.europa.eu)
- Valanto, P., Soukup, P. (2016). Studie zum Verhalten eines Mehrzweckarbeitsbootes für die Bundesanstalt Technisches Hilfswerk (THW) [Investigation on the Behavior of a Multi-Purpose Workboat for the Federal Agency for Technical Relief (THW)], HSVA-Bericht No. 1684. [www.hsva.de](http://www.hsva.de).
- Wigton, L. (1979) Glimm's Method for Humans, Lecture Notes prepared for course on numerical methods, Department of Mechanical Engineering, University of California, Berkeley.
- Zhou, Z.Q., De Kat, J.O., Buchner, B. (1999). A Nonlinear 3-D Approach to Simulate Green Water Dynamics on Deck, 7th International Conference on Numerical Ship Hydrodynamics. 15 p.

## 7.5 Annex E: aNySIM software

### Introduction

The first time domain simulation tool that was developed at MARIN for the use of damage ship stability survivability assessment was developed within the Cooperative Research Navies (established in 1989), and denoted FREDYN (fregat dynamics). The source code and theory manual is confidential to the CRN as the manoeuvring model is a unique dedicated one for Navy ships.

The FREDYN code was developed to capture the ship dynamics while sailing (at speed) under severe weather conditions, studying both intact as well as damage stability issues. For that purpose a seakeeping and manoeuvring model were combined in a unified model.

The CRN objective is to use FREDYN for risk assessment; De Kat et al. (1994). Next to the nacy application, FREDYN was used as well for many other ship types in for example to predict the risk on parametric roll of containerships, France et al. (2001).

When the flooding module matured around 2000, MARIN become involved in the damage stability assessment of large cruise ships through IMO and EU projects and ITTC benchmarking; see e.g. Van 't Veer and de Kat (2000), De Kat and Van 't Veer (2001), Ypma and Turner (2010).

In later phase, MARIN developed the aNySIM simulation tool for zero speed offshore application. This package is nowadays implemented on the so-called XMF platform of MARIN. This platform assures that all time domain simulation tools have a common basis. Nowadays, FREDNY and aNySIM share the same ship hydrodynamic solvers, where FREDYN is traditionally used on the basis of 2D strip theory, aNySIM is based on hydrodynamic coefficients from a 3D panel code.

The original flooding model of FREDYN is based on the Bernoulli flow principle and applies tank-tables to know at each time step the centre of mass of the floodwater and its inertia properties. These tank-tables are generated by e.g. PARAMARINE, which is unfortunately a not so user friendly program for this purpose.

Recently, a Unified Internal Flow model is developed (UIF). Motivation for this development was to include fluid inertia terms into the equation to model for example the motions of an anti-roll tank. The UIF model is developed in-house and not within the CRN working group. It can be used in combination with FREDYN or in combination with aNySIM. The latter combination will be used in the FLARE project.

The UIF model utilizes geometrical objects (OBJ/STL objects) that prescribe the tank volume at each time instance. Tank tables are not required anymore. This is a huge benefit for the user.

The UIF model is currently under verification and validation for application in FLARE. It has been tested on anti-roll tanks, moonpools and other simple flooding configuration successfully, such as demonstrated in Figure 4-6.

## Development of the time domain solver

MARIN has been developing, using and selling hydrodynamic simulation software for many decades. Well-known predecessors of aNySIM XMF are TERMSIM, LIFSIM, DPSIM, DREDSIM and DYNFLOAT.

aNySIM XMF is used by engineering companies, oil companies, ship yards, consultants and contractors. MARIN also uses aNySIM XMF for most engineering studies at zero or low speed.

aNySIM XMF is part of the Extensible Modelling Framework (XMF). XMF is a software toolkit on which all MARIN's fast-time and real-time simulation software is based. The XMF development focuses on object interoperability, reusability, extensibility, and Newtonian dynamics. The modular approach makes the software flexible in use.

## aNySIM Numerical model

The numerical model solves the 6-DOF motion equation using:

- Non-linear hydrostatics
- Non-linear wave excitation on the actual wetted hull surface
- Linear wave-radiation loads through convolution integrals
- Linear diffraction loads through RAO's
- First and second order wave loads (drift loads)
- Springs between body-earth or between rigid bodies (multi-body approach)
- Various user defined forces, DP, wind, current, etc
- Interaction with flooding loads from the UIF model

## Unified Internal Flow (UIF) model

The Unified Internal Flow (UIF) model can be executed in two different modes: a) following the steady Bernoulli flow equations (Torricelli-law), b) following a 3D cell-averaged momentum balance in combination with a 1D flow between compartments.

Water ingress/egress is based on Bernoulli's equation with associated flow loss coefficients specified for each opening. The discharge coefficients are user input and can be defined per opening.

The internal spaces (floodable area's) are described by OBJ/STL geometry objects which can have any shape.

The UIF model calculate at each time step, once an object is flooded, the volume, centre of mass and the fluid inertia properties. The water surface in each floodable object remains earth-fixed. Using multiple objects in "a single tank volume" the progression of water on large open decks can be modelled. The shallow water properties are approximately obtained.

While the FREDYN flooding model has been used extensively over the past 20 years and has been used in many studies, such as the ITTC benchmarking, the present UIF model used for

FLARE has not yet seen such utilization. The UIF model has a more generic approach and is preferred therefor. It utilizes for example a graph solver to account for air compression effects between adjacent compartments. An SVD solver is used to calculate the flow properties between compartments in a two-step approach. First the unconstrained flooding process is solved after which the constraint solver modifies the solution based on for example the constraint of a compartment becoming completely full or empty within one time step. This assures a robust implementation of the complex flood water flow through the ship.

The UIF model can model frictional losses by means of user defined energy loss in the tanks or by user defined frictional losses on the openings (discharge coefficients).

## References

Van 't Veer, R., de Kat, J.O. (2000): "Experimental and Numerical Investigation on Progressive Flooding and Sloshing in Complex Compartment Geometries", Proc. 7<sup>th</sup> International Conference on Stability of Ships and Ocean Vehicles (STAB2000), 7-11 February, Launceston, Tasmania, Australia, pp. 305-321

De Kat, J. O., Brouwer, R., McTaggart, K.A., and Thomas, W.L. (1994): 'Intact ship survivability in extreme waves: New Criteria From a research and naval perspective'. Fifth International Conference on Stability of Ships and Ocean Vehicles, STAB '94 Conference, Melbourne, Florida, Nov. 1994.

De Kat, J.O. and Van 't Veer, R. (2001): Mechanisms and physics leading to the capsize of damaged ships, Proc. 5<sup>th</sup> Int. Ship Stability Workshop, Trieste, September 2001

Ypma, E., Turner, T. (2010): "An Approach to the Validation of Ship Flooding Simulation Models", Proc. 11<sup>th</sup> International Ship Stability Workshop (ISSW2010), 21-23 June, Wageningen, The Netherlands, pp. 173-184

France, W. N., Levadou, M., Treacle, T. W., Paulling, J. R., Michel, R. K., Moore, C. (2001): An Investigation of Head-Sea Parametric Rolling and its Influence on Container Lashing System, SNAME Annual Meeting 2001



## 7.6 Annex F: Hull breach

(Author: Dr. Petri Valanto and Dr. Ing. Weede, HSYA 06/09/2019)

### On the evaluation of the opening time of a collision damage for water flow caused by a perpendicular collision between two ships

Let us assume a collision as in Figures 1 and 2 has taken place. Figure 3 shows consequences of such a collision in reality.

For flooding simulations in time domain it is important to know how fast can water flow into the damaged ship through an inlet or breach in the hull. For this it is relevant to know the opening process of the inlet. It can be assumed that the breach leaks along the damage boundary from the onset of the damage, that is, from the very beginning. However, in comparison to the whole area of the breach, this boundary area available for initial water ingress from the beginning is likely to be considerably smaller.

For transient flooding simulations it is relevant at which rate the opening on the ship side becomes free for water ingress. The magnitude and duration of the impulse of the ingress water on the ship depend on this opening rate, and so does the heeling reaction of the ship.

It can be assumed that in many cases the ship bow stays in the damage and the water flow through it is only relatively gradual. *In a collision case it is not possible that the ship bow just disappears and the inlet or breach on the hull suddenly becomes 100 percent fully open. However, it cannot be excluded that the ship, which penetrated the other ship, applies full available thrust astern to free itself from the other ship for whatever reason. This means that the ship accelerates from the state of standstill and moves astern the distance it had penetrated the other ship. During this movement the area of the hull breach or the damage inlet becomes free for water flow as it is not anymore blocked by the ship bow. This scenario is perhaps the fastest possible way the damage opening can become free for water flow, and thus should represent a plausible minimum opening time.*

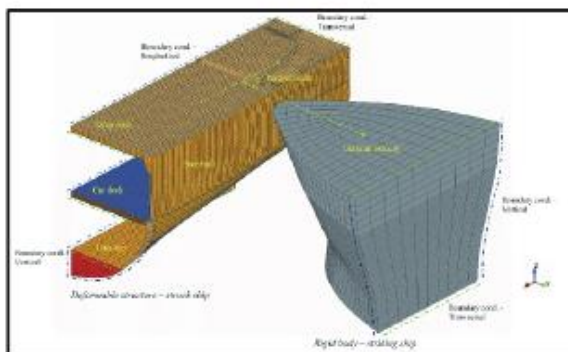


Figure 1 Ship to ship collision.

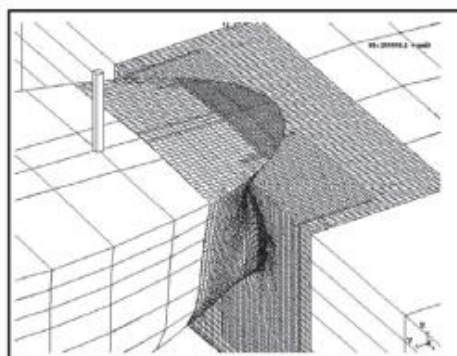


Figure 2 Ship to ship collision.



Figure 3 Ship to ship collision damage.

The growth of this area can be coarsely evaluated as follows: The sectional area curve of the ship gives the areas of the submerged vertical sections or frames at any given location along the ship length. See Figure 4.



**Figure 4** Sectional area curve of a ship.

Let us assume that the final penetration length is  $d_x$ . At this penetration length  $d_x$  taken from the tip of the ship bow the curve gives the final sectional area  $A_D$  of the bow of the striking ship, at the cross-section defined by the vertical side of the other struck, damaged ship.

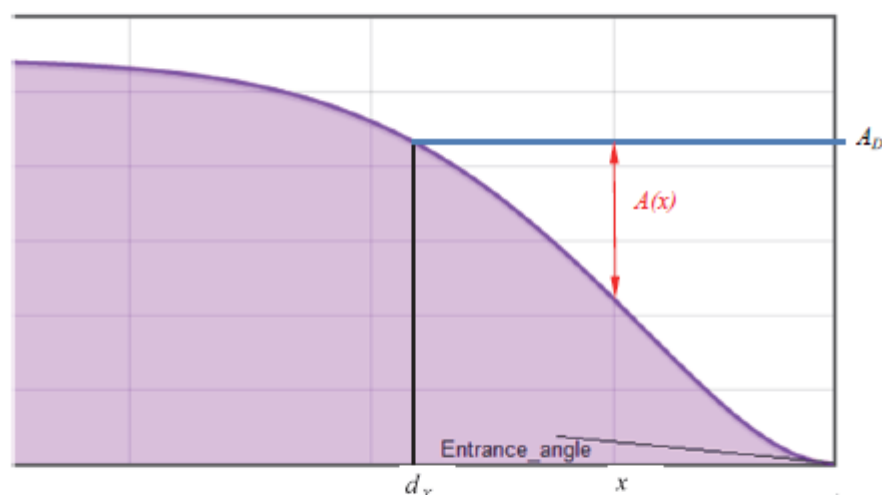


**Figure 5** Presentation of the area  $A(x)$  becoming free when the ship pulls back from the damage. The damage opening becomes gradually free for water flow as the ship bow starts to move astern. The difference  $A(x)$  in Figure 5 between the  $A_D$  and the area under the ship sectional area curve at given  $x$  position gives the area not blocked by the ship bow, but

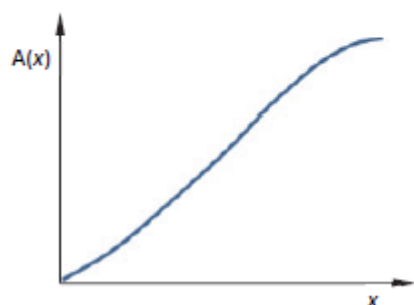


**Figure 6** Area  $A(x)$  becoming free as the ship pulls back from the damage.

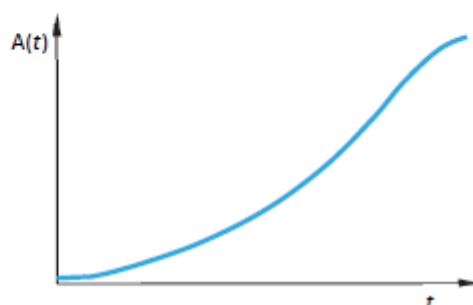


**Figure 7** Development of the area  $A(t)$  becoming free as a function of time.

2

open for the water ingress into the damaged ship. The coordinate  $x$  is zero at the beginning and it reaches the final penetration length  $d_x$  at the end. The area  $A(x)$  is shown anew in Figure 6.

With some basic knowledge of ship powering it is possible to estimate the time needed for the ship to move this distance astern. With this approach one can obtain a curve as shown in Figure 7, which can be used as an input in the time domain simulations for ship flooding. As the ship starts to move from standstill, the growth of the damage opening will be slow in the beginning.

In order to get some realistic insight and information on such collision damage openings, the following investigation was carried out:

In order to start we assume B/5 damage on the side of the struck ship, that is, this is the assumed penetration depth. This value is based on SOLAS Reg. II-1/B/8.4.2. The following common five widths of the damaged ships will be studied:  $B = 23, 27, 32, 36,$  and  $47$  m. Thus the penetration depths to be investigated become  $4.6, 5.4, 6.4, 7.2,$  and  $9.4$  m.

Altogether 10 different ships striking into the other ship's side will be investigated on their astern motion from standstill in the final damage position based on their mass, resistance and thrust astern available at pollard pull/near bollard pull conditions. For each penetration depth the development of the damage opening as a function of time can be plotted for each of the 10 ships. The calculation procedure with details is outlined in Appendix 1.

## Results

For the start the astern motion as a function of time for ten ships is shown in Figure 8.

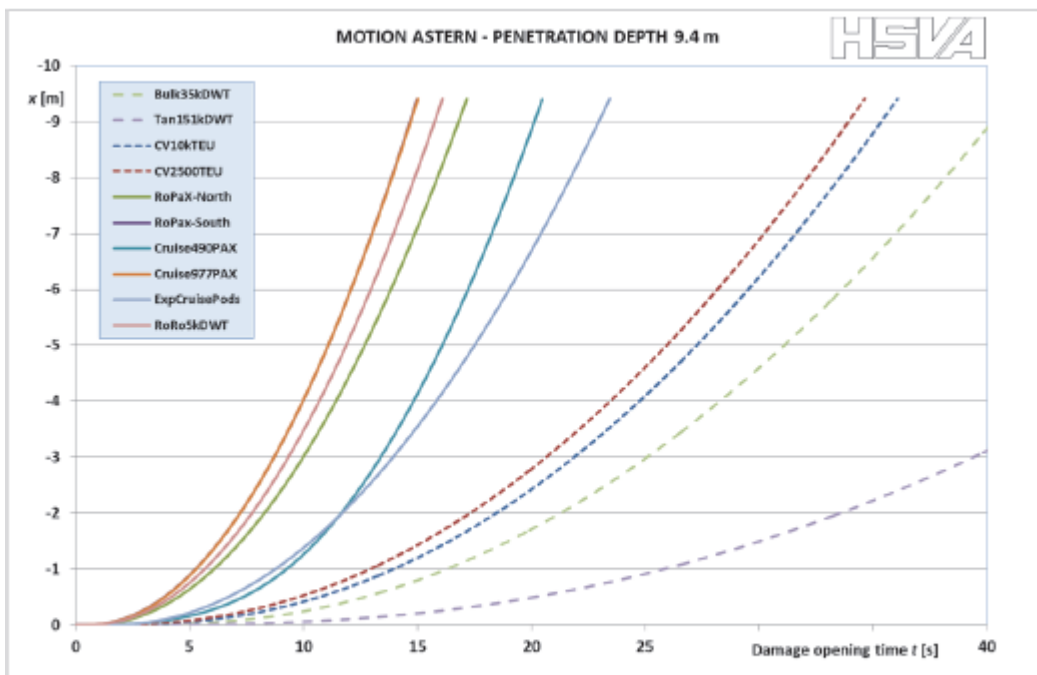


Figure 8 Ship motion astern as a function of time for ten typical ships. Details in Appendix 1.

We can see in Figure 8 that the curves are very smooth and that, with some goodwill, there appears to be two groups of ships, namely in one group Cruise Ships, RoPaX and Roro ships and in the other Container Vessels, Tankers and Bulkers. This should not be surprising considering the propulsion arrangements and propulsion power of these ship types.

Figures 9 and 10 show the development of the relative open damage area  $A(t)/A_D$  and the  $A(t)$  in m<sup>2</sup> as a function of time for the same ships for the penetration length 9.4 m. The curves show also the changes in the hull form and in the sectional area curve of each ship.

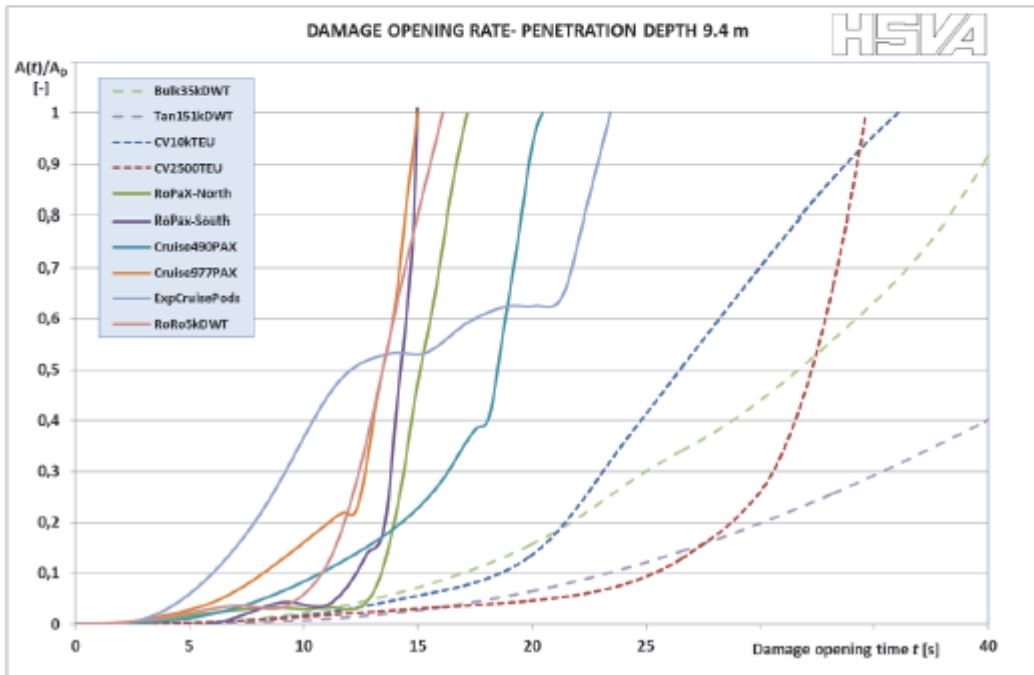


Figure 9 Damage opening size as a function of time. The relative damage area  $A(t)/A_D$  is shown.

The two ship groups appear also in Figure 9 but less in Figure 10, as the large slow moving ships show also a large rate of change in the sectional area: Thus even relatively small motion astern causes significant changes in  $A(x)$ , and thus also in  $A(t)$ . Figures 11 and 12 show the development of the open damage area for the same ships for the penetration length 4.6 m. The two groups are more close together.

Before we consider what these curves mean for the damage opening times and their relevance in numerical or physical modeling of the ship roll or heeling motion, we should keep in mind that the roll RAO shape is a relatively narrow high peak around the natural roll period of the ship. Thus the ship roll motion will be most easily excited if the exciting force or moment fluctuates with the natural frequency or period of the roll motion.

If the exciting heeling moment is not sinusoidal, this 'resonant' dynamic roll response of the ship should be most easily excited when the exciting moment has a rise time of half a roll period  $T/2$ .

Many cruise ships appear to have a roll period between 19 and 27 seconds, many RoPaX ships between 13 and 20 s. The corresponding half periods  $T/2$  for best roll excitation as above

become 9.5-13.5 s and 6.5 - 10 s for cruise ships and RoPax ships, respectively. These time spans are also quite near the time spans in Figures 9 to 12 during which the damage opens quite rapidly, if the striking ship was another passenger vessel or RoRo. If the striking ship was a

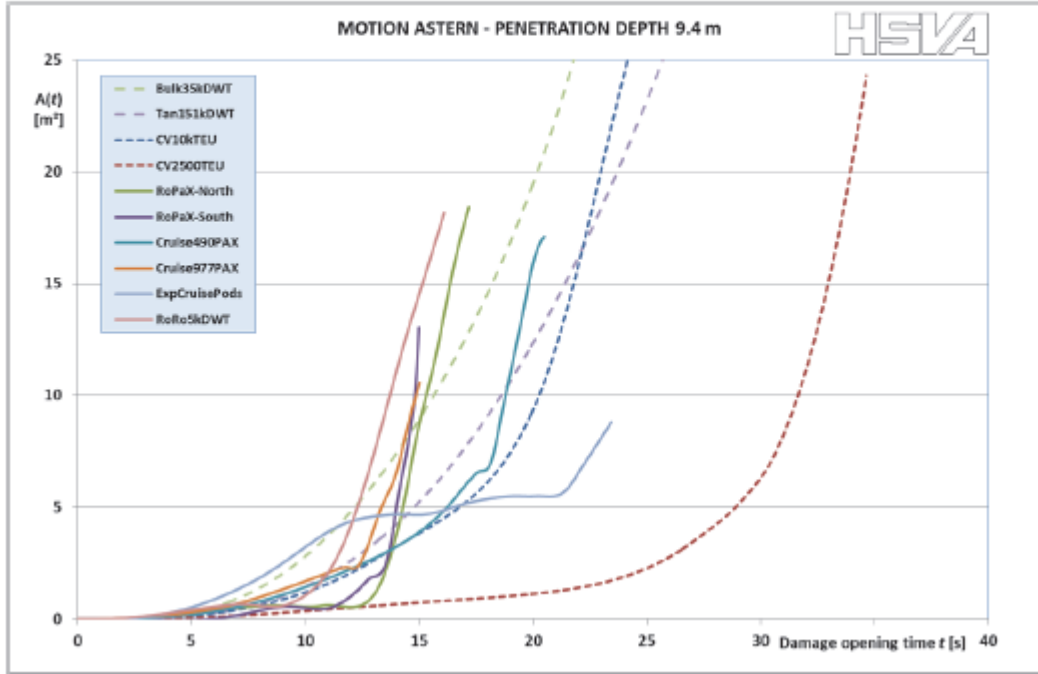


Figure 10 Damage opening size as a function of time. The damage area  $A(t)$  is shown.

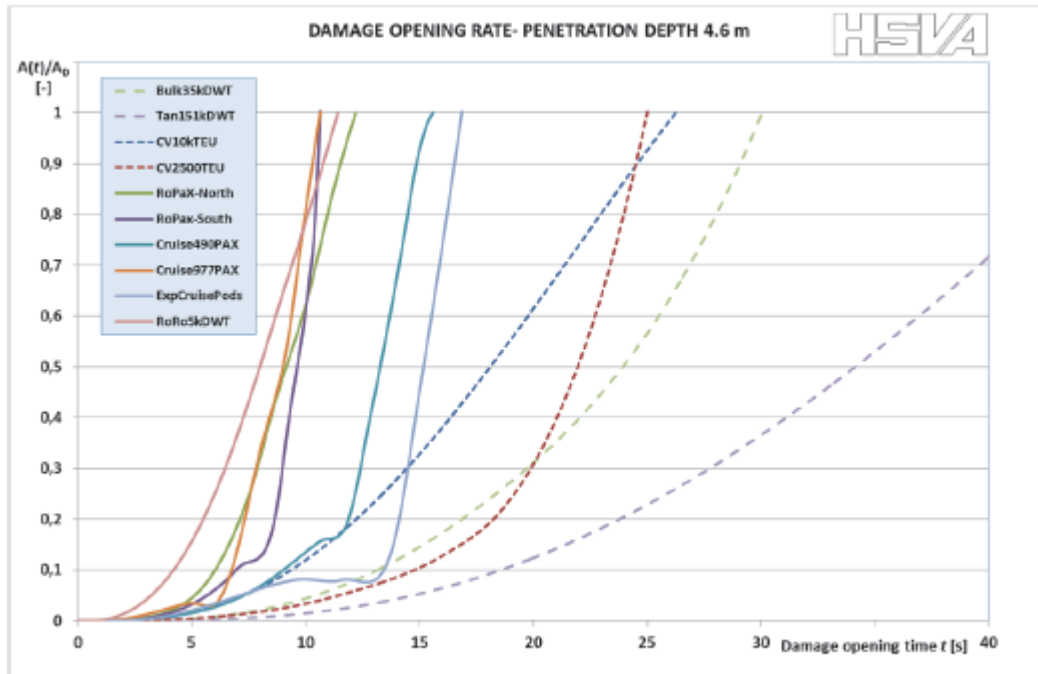


Figure 11 Damage opening size as a function of time. The relative damage area  $A(t)/A_0$  is shown.

container vessel, tanker or bulker the rate of damage opening depends on the ship size. Note that the given time span values in question are not the values of the damage opening times along on the x-axis starting from zero, but any time-intervals in which the damage opening grows significantly. Physically these time intervals with a high rate of damage opening are often related to the tip of the ship bulb being pulled out of the damage hole at the moment when the ship has already gained some speed. Prior to this moment in time the speed is slower and the sectional area of the ship underwater hull shows only more gradual changes. If the final penetration depth is larger as shown in Figure 10, the speed astern when the round tip of the bow is pulled out of the damage is higher than in case of smaller penetration depth shown in Figure 12, in which case the ship had less time to gain speed astern. This is clearly visible in Figures 10 and 12.

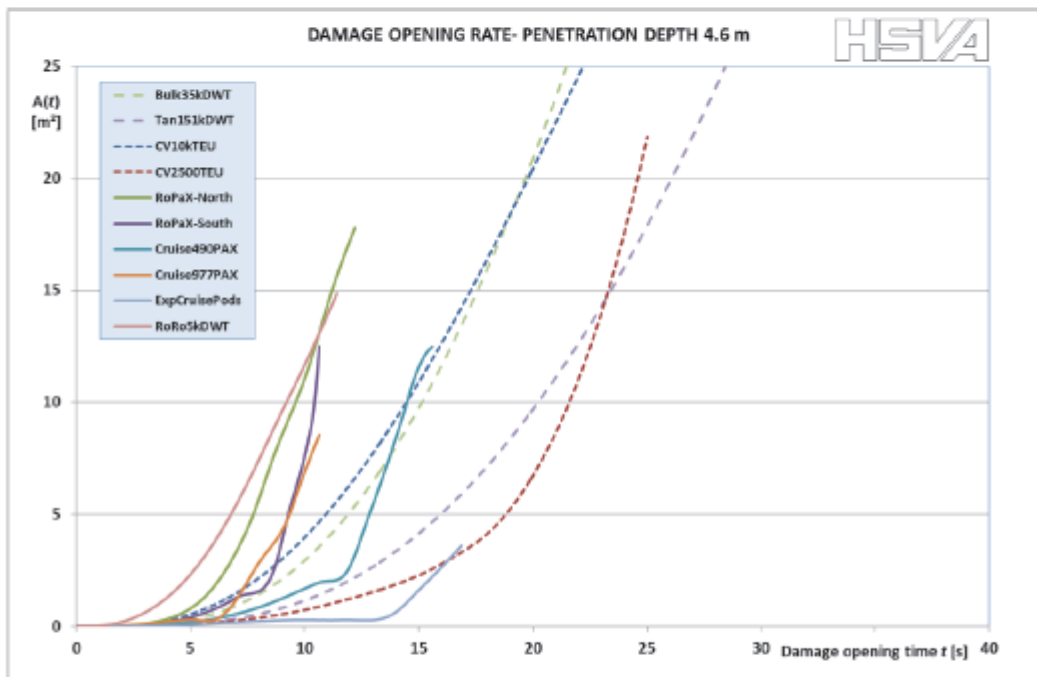


Figure 12 Damage opening size as a function of time. The damage area  $A(t)$  is shown.

### Discussion

Everything in this paper ignores any hindrances to open flow in the damaged ship itself, like debris, broken cabins etc. It is also possible that the striking ship does not pull back, and the damaged compartments fill up slowly. Second, it is not clear at which power level the ship would pull back. We have used here the assumption of full astern, as this cannot be closed out, e.g. in case of fire or doubt on it. Thus the damage opening rate and the water ingress can always be slower than in our calculations. Can, but does not have to be. Note also the quite clean, open hole at the side of a damaged ship in Figure 3. Although the important rise time of the heeling moment due to sudden water ingress is not exactly equal to the calculated damage opening time, they should be very closely related. Following conclusions can be drawn:

- Plausible estimates for minimum damage opening times were obtained: It is very easy to extend the calculation to further penetration depths, if needed.

- There appears to be some collision cases, in which we do not have to consider transient flooding, as the opening rate of the damage is likely to be relatively slow, particularly in view of the internal subdivision of the struck ship.
- For some (striking) ship hull forms the instant opening of the damage inlet, often approximately the size of the cross section of the penetrated bulb of a ship, appears as a plausible simplification, for some other hull shapes and damage sizes not. Much depends on the local underwater shape of the bow. If less than full astern power is applied to withdraw the ship, the slower the motion and the less suitable the simplification of the sudden opening is.
- If we model the transient heeling due to rapid water ingress numerically, we should try to model the opening rate of the damage. Its effect cannot be closed out and an instant opening may not be the worst case, as the ingress water may spread evenly on the ship before the ship reacts with heeling. This should be relevant for ships with large open spaces behind the damage.
- The effect of the opening rate of the damage, e.g. versus instant opening, on the ship survivability can easily be investigated with numerical models.
- A prolonged initial slow water ingress before sudden pull out of the ship bow would influence the pressure head in the damage opening at pull out, and thus the water ingress.
- With such relatively simple calculations as in this paper in Appendix 1 it should be possible to limit the number of cases, in which a potentially dangerous transient flooding can take place. This can have an effect on the general (estimated) fleet survivability in a ship to ship collision damage case.



## Appendix 1: Estimation of the opening time of a collision damage through withdrawal by accelerating full astern

This study deals with the ship which struck another ship. The other damaged ship is not investigated, but should be imagined as a hypothetical deep vertical wall with a damage hole. For 10 typical ships, the full astern acceleration was simulated. Assuming that this acceleration takes place to pull the ship bow out of a collision damage in another struck ship starting from a given penetration depth, the collision damage area on the side of the struck ship open to water flow was determined from ship motion astern as a function of time and the cross-sectional area curve of the ship.

### Selection of typical ships

A database with all HSVA ship models was used. All model numbers above 4000 were considered, altogether about 1400 ships. This model number range approximately corresponds to the model tests since the beginning of this millennium. The most frequent ship type categories were extracted from this material. All container vessels were subdivided into those longer and those shorter than the mean length of container vessels. The same subdivision was performed for bulkers and tankers. Thus, the ships were subdivided into following groups, where FPP means fixed-pitch propellers and CPP means controllable pitch propellers:

- Smaller container vessels, single-screw with FPP and combustion engine
- Larger container vessels, single-screw with FPP and combustion engine
- Smaller bulkers and tankers, single-screw FPP and combustion engine
- Larger bulkers and tankers, single-screw with FPP and combustion engine
- Ropax and RoRo vessels, twin-screw with CPP and combustion engines
- Cruise vessels, twin-screw with CPP, or podded drives with FPP and electrical engines

Multiple occurrences of the same model within one group were eliminated by two criteria: Only the largest model index was considered assuming that this probably describes the final version, and only the largest draught was considered.

Thereafter each group was sorted in a manner that the most typical ships appear on top of the list. For this, for each of several parameters the difference to the mean value of all ships within the group was expressed as ratio to this mean value, e.g. for the length  $\varepsilon_L = (L - L_{MEAN}) / L_{MEAN}$ . These ratios were combined to one single magnitude  $\varepsilon = \sqrt{(4\varepsilon_L^2 + 3\varepsilon_V^2 + 2\varepsilon_{PD}^2 + \varepsilon_{CB}^2 + \varepsilon_{L/B}^2 + \varepsilon_{B/T}^2)} / 12$  representing the length  $L$ , displacement volume  $V$ , nominal propulsion power  $P_D$ , block coefficient  $C_B$ , length/breadth ratio  $L/B$  and breadth/draught ratio  $B/T$ . The most typical ships within each group have the smallest  $\varepsilon$  values and appear on top. From each group one or several ships were selected from the most typical ones on the top.

### Overview of the input data

The ten ships resulting from the selection process were given unique symbols used throughout this analysis. The following tables show all input data to approximately simulate the astern acceleration out of the damage:

**Table 1** Input data, part 1 of 3.

Symbol	Type	Lpp	B	T	LCB	Displacement volume
[-]	[-]	[m]	[m]	[m]	[m]	[m <sup>3</sup> ]
CV2500TEU	Container Vessel, 2500 TEU	186.4	29.8	11.55	87.552	43037
CV10kTEU	Container Vessel, 10 000 TEU	319	48.6	14.5	155.26	149581
Bulk35kDWT	Bulker, 35 000 DWT	169.7	29.5	10.4	89.126	42968
Tan151kDWT	Tanker, 151 000 DWT	258	46	16.2	138.185	156674
RoRo5kDWT	RoRo, 5000 DWT	138	24	6.5	63.094	14224
RoPax-North	RoPax	152.43	30	6	69.267	17280
RoPax-South	RoPax	158.24	21.9	5.55	74.409	11842
Cruise490PAX	Cruise Ship, 490 passengers	159.11	24.12	7.5	67.843	19000
Cruise977PAX	Cruise Ship, 977 passengers	139.83	22.5	5.4	63.506	10909
ExpCruisePods	Expedition Cruise Ship, pod drives	133.5	23.6	5.3	60.16	11281

**Table 2** Input data, part 2 of 3.

Symbol	Nominal speed	Nominal power	Nominal revolution rate	Engine type
[-]	[kts]	[kW]	[rpm]	[-]
CV2500TEU	22	19810	108	combustion
CV10kTEU	23.5	58100	84	combustion
Bulk35kDWT	14.2	6400	110	combustion
Tan151kDWT	15.4	18660	91	combustion
RoRo5kDWT	21	16800	155	combustion
RoPax-North	21	15650	120	combustion
RoPax-South	22.5	17172	215	combustion
Cruise490PAX	19.5	21000	120	electric
Cruise977PAX	21	14000	185	electric
ExpCruisePods	15	6500	169	electric

**Table 3** Input data, part 3 of 3.

Symbol	Number of propellers	Propeller type	Number of blades	Propeller diameter	Pm/D	Ae/A0
[-]	[-]	[-]	[-]	[m]	[-]	[-]
CV2500TEU	1	FPP	5	6.8645	0.944	0.61
CV10kTEU	1	FPP	6	9.5	0.9488	0.7131
Bulk35kDWT	1	FPP	4	6	0.7016	0.4823
Tan151kDWT	1	FPP	4	8.3	0.7199	0.7501
RoRo5000DWT	2	CPP	4	4.5	1.1455	0.65137
RoPax-North	2	CPP	4	5.2	1.20893	0.55669
RoPax-South	2	CPP	5	3.8	1.05956	0.83136
Cruise490PAX	2	CPP	4	4.6	1.1455	0.65137
Cruise977PAX	2	CPP	5	4	0.92631	0.68999
ExpCruisePods	2	FPP	4	3.3	1.1183	0.5182

### Simulation of the acceleration astern

The angular momentum theorem of the total rotating equipment (propeller, shaft, rotating engine parts) was used within two different algorithms:

- During the pressure air starting process, the angular momentum theorem serves to calculate the angular acceleration from the given constant engine torque. The differential equation is integrated using the difference method

$$\Delta n = \frac{\sum Q}{2\pi I_{xx}} \Delta t \quad ,$$

where  $n$  is the rate of propeller revolutions,  $\sum Q$  is the superposition of engine and propeller torque.

- At normal mode of operation (no pressure air starting), the angular momentum theorem serves to add the inertia effects from the equipment's angular acceleration to the propeller torque to find the required engine torque. This is done within a binary search loop to find the largest possible increment of lever position limited by three criteria: the available engine torque corresponding to the revolution rate, cavitation, and the maximum rate of change of lever position. Each lever position defines a combination of revolution rate and pitch angle in case of CPP or simply a revolution rate in case of FPP.

Within an outer loop around all this, the momentum theorem of astern surge motion is solved numerically with the difference method

$$\Delta v = \frac{\sum X}{(1+c_A)\rho v} \Delta t \quad ,$$

where  $v$  is the ship speed,  $\sum X$  the sum of resistance and system thrust,  $c_A$  is the added mass coefficient. A second numerical integration  $\Delta x = v \Delta t$  thereafter determines the travelled distance  $x$  based on the momentary speed.

Missing detail data were replaced by following assumptions:

#### Resistance and propulsion data

Resistance and propulsion tests astern are generally not carried out, and no such data for the ships are available. Instead, this empirical formula derived from captive tests for dynamic positioning (DP) was used for the astern resistance at low speeds:

$$|R_r| = \left( -0.96265 + 0.02983232 \frac{L}{B} + 0.08649535 \frac{B}{T} + 0.9274514 c_B + 0.569742 \frac{x_G}{L} \right) \frac{\rho}{2} v^2 B T$$

where  $L$  is the length between perpendiculars,  $B$  the breadth,  $T$  the draught,  $v$  the ship speed,  $x_G$  the centre of buoyancy in front of the main section, and  $c_B$  the block coefficient. Please note that no influence from the penetrated, damaged ship is considered, neither hydrodynamic suction or possible reduced hydrostatic pressure at the bow, nor mechanical forces arising from the separation of the two structures crunched into each other. Any such forces would slow down the astern motion of the ship and prolong the damage opening rate at the side of the struck ship. Thus calculated results represent a plausible minimum.

In order to determine the propeller's inflow velocity  $v_A$  from the ship speed  $v$  as  $v_A = (1-w)v$  the Taylor wake fraction  $w$  is required. The transformation of the propeller thrust  $T$  into its surge force contribution  $X$  as  $X = (1-t)T$  requires the thrust deduction fraction  $t$ . In case there is a lack of astern resistance and propulsion test data for any ship, the  $w$  and  $t$  are estimated for the astern motion as follows:

**Table 4** Taylor wake fraction and thrust deduction values.

	Taylor wake fraction $w$	Thrust deduction fraction $t$
single-screw vessels	0	0.15
twin-screw vessels		0.05

### Propeller characteristics

When accelerating astern, fixed pitch propellers work in the third quadrant, and controllable-pitch propellers in the fourth quadrant of the advance angle. Propeller test data are not available for such unusual cases. Therefore, an approach based on the four-quadrant formulae for Wageningen B propellers published by Roddy, Hess and Faller [1] was used. In that reference, the four-quadrant thrust coefficient  $c_T$  and torque coefficient  $c_Q$  are expanded into Fourier series of the advance angle  $\varepsilon$ :

$$c_T(\varepsilon) = \frac{T}{\frac{\rho}{2}(v_a^2 + (0.7\pi nD)^2)\frac{\pi D^2}{4}} \quad c_Q(\varepsilon) = \frac{Q}{\frac{\rho}{2}(v_a^2 + (0.7\pi nD)^2)\frac{\pi D^3}{4}}$$

$$\varepsilon = \begin{cases} \arctan \frac{v_a}{0.7\pi nD} & \text{if } n \geq 0 \\ \arctan \frac{v_a}{0.7\pi nD} + \pi & \text{if } n < 0 \end{cases}$$

Where  $T$  is the thrust,  $Q$  the torque,  $v_A = (1-w)v$  the axial inflow velocity,  $n$  the revolution rate,  $D$  the propeller diameter,  $\rho$  the water density. Fourier coefficients are presented in that reference for many different combinations of mean pitch ratio  $P_m/D$ , disk area ratio  $A_d/A_0$  and number of blades. With a poly-dimensional spline interpolation among these three parameters an algorithm derived from that reference is able to model also propellers not matching exactly one of the Wageningen B propellers, as far as it is a fixed-pitch propeller. For a controllable-pitch propeller with astern pitch, one can assume that it behaves more or less like the corresponding fixed-pitch propeller running ahead, but with the torque coefficient  $c_Q$  1.5 times as large. The relation between the pitch angle  $\alpha$  from the design pitch and the change of mean pitch ratio  $P_m/D$  is approximately

$$\alpha = \frac{\Delta P_m / D}{0.7\pi} .$$

The method to approach astern pitch angle by a corresponding Wageningen B propeller with fixed pitch and rotating astern is applied up to the smallest pitch covered by the Wageningen B propellers. Around the zero thrust pitch angle, an interpolation between the ahead and the astern mathematical models takes place.

#### Maximum astern pitch angle for controllable pitch propellers

This magnitude is not contained in the used database, and asking the manufacturers would be far outside the capacities of this project. Therefore, a default value has to be estimated. Using the nominal revolution rate from the database and the corresponding maximum possible engine torque or power at that revolution rate from the engine characteristics, a steady astern motion was simulated at various astern pitch angles to find the extreme case where the required torque or power matches the maximum possible one.

#### Combination of revolution rate and pitch

Controllable pitch propellers require mapping the two control signals – pitch angle and revolution rate – into one single control signal, the lever position. This is performed by combinator curves or tables defining one combination of ahead revolution rate and ahead or astern pitch angle for each lever position between full astern and full ahead. It is strongly recommended not to use the combinator curves from the manufacturer, because these are made for transit conditions and would cause an engine stall of combustion engines when abused for crash stop or astern acceleration. Instead, a high revolution rate at all ahead and astern pitch angles is necessary. We built a default combinator table by these four states with the nominal power  $P_{nom}$  and maximum power  $P_{max}$  and the revolution rate resulting from steady motion astern or ahead:

**Table 5** Sense of rotation.

Sense of rotation	power	pitch angle	lever
astern	$P_{max}$	extreme astern	-1
astern	$P_{nom}$	extreme astern	$-P_{nom}/P_{max}$
ahead	$P_{nom}$	0 (design pitch)	$+P_{nom}/P_{max}$
ahead	$P_{max}$	0 (design pitch)	+1

When using this table during time domain simulation of the astern acceleration, the pitch angle and revolution rate corresponding to any lever position is found by linear interpolation among these four data points.

#### Engine characteristics

Such data were not available in the database. Just a nominal power and nominal revolution rate are available. We assume that up to the nominal revolution rate combustion engines can produce a maximum torque linearly increasing with the revolution rate, and electrical engines a constant torque. And we assume that beyond that point, the maximum engine power is constant. However, combustion engines cannot run slower than some minimum revolution rate and thus not be described by such engine characteristics when starting from

zero. Instead, a pressure air starting process is required. We assumed that the pressure air provides a constant torque for any revolution rate which amounts 0.8 times the nominal torque of the engine. Where necessary, we modified this torque by hand. It was assumed that the pressure air starting process is stopped as soon as the revolution rate reaches the value where the maximum feasible torque of the running engine matches the air pressure torque. In cases where this resulted in an unrealistically short duration of the starting process, we modified the pressure air torque. For simplicity we neglected an initial time ramp and assumed that the full pressure air torque acts immediately. Such pressure air starting process was only considered for fixed-pitch propellers. For controllable-pitch propellers it was assumed that at the beginning of the motion simulation the propellers are running with zero-thrust pitch angle and the corresponding revolution rate following from the combinator table.

#### Further default values

The added mass coefficient of surge motion was estimated from literature and is small. The moment of inertia  $I_{xx}$  of a propeller including added mass, of the shaft and the engine was estimated from the propeller diameter  $D$  as  $I_{xx} = 21 \text{ kg} / \text{m}^3 D^5$ . The minimum duration from full ahead to full astern was assumed to be merely 5s to obtain a pessimistic (fast) estimation of the motion. Actually, this is only a theoretical magnitude, because most of the time the real rate of change of the propeller revolution rate and pitch is governed by the maximum available engine torque. As the database contains only the nominal power of the ship, the maximum available power was assumed to be 1/0.85 as large.

#### Open part of the damaged area

The time domain simulation yields the surge motion  $x(t)$  of the coordinate origin in the main section, with the direction being astern and thus negative. Thereafter, this is combined with the sectional area curve  $A(x)$  expressing the section area  $A$  depending on the distance  $x$  from the main section and available as data table. The wetted part of the ship hull ends at  $x_{max}$ , where  $A(x_{max}) = 0$ , and which has initially penetrated into the other, struck ship by the penetration depth  $d$ .

The open part of the damage has the area  $\Delta A$ , which increases with time according to the function

$$\Delta A = A(x_{max} - d) - A(x_{max} - d + |x(t)|) .$$

#### Results

Each of the ten ships was analysed with the initial penetration depths 4.6m, 5.4m, 6.4m, 7.2m, and 9.4m. The resulting time series are available as csv- files, with names like ExpediPods-64.csv, i.e. the ship's symbol and ten times the penetration depth. They have been calculated with a time step of 0.01 s and contain the following columns:

**Table 6** List of data columns in data files.

$t$	[s]	Time
$x$	[m]	surge motion
$v$	[kts]	Speed
$n$	[rpm]	revolution rate

pitch	[deg]	pitch angle from design pitch
$P_D$	[kW]	actual engine power (all engines)
$P_{D,lim}$	[kW]	available engine power (all engines)
phase	[-]	1=normal, 3=pressure air starting
$A$	[m <sup>2</sup> ]	open part of the damaged area
$t'$	[-]	non-dimensional time $t/t_{max}$
$A'$	[-]	ratio of open part to total damaged area

The results can be condensed to one table where the total damaged area and the duration of opening are shown for each combination of ship symbol and penetration depth.

**Table 7** Condensed results.

Damage Depth	4.6 m	5.4 m	6.4 m	7.2 m	9.4 m
CV2500TEU	21.84 m <sup>2</sup> / 25.01 s	22.59 m <sup>2</sup> / 26.88 s	23.14 m <sup>2</sup> / 29.04 s	23.35 m <sup>2</sup> / 30.64 s	24.31 m <sup>2</sup> / 34.64 s
CV10kTEU	33.22 m <sup>2</sup> / 26.26 s	41.39 m <sup>2</sup> / 28.17 s	53.36 m <sup>2</sup> / 30.36 s	60.95 m <sup>2</sup> / 31.99 s	68.74 m <sup>2</sup> / 36.05 s
Bulk35kDWT	67.05 m <sup>2</sup> / 30.05 s	76.17 m <sup>2</sup> / 32.18 s	86.31 m <sup>2</sup> / 34.64 s	97.705 m <sup>2</sup> / 36.48 s	123.80 m <sup>2</sup> / 41.05 s
Tan151kDWT	78.16 m <sup>2</sup> / 47.01 s	94.78 m <sup>2</sup> / 50.27 s	116.73 m <sup>2</sup> / 54.00 s	135.43 m <sup>2</sup> / 56.78 s	190.62 m <sup>2</sup> / 63.70 s
RoRo5kDWT	14.87 m <sup>2</sup> / 11.42 s	16.50 m <sup>2</sup> / 12.33 s	17.47 m <sup>2</sup> / 13.37 s	17.57 m <sup>2</sup> / 14.15 s	18.16 m <sup>2</sup> / 16.10 s
RoPax-North	17.78 m <sup>2</sup> / 12.21 s	17.81 m <sup>2</sup> / 13.18 s	17.86 m <sup>2</sup> / 14.29 s	17.78 m <sup>2</sup> / 15.11 s	18.40 m <sup>2</sup> / 17.18 s
RoPax-South	12.49 m <sup>2</sup> / 10.64 s	12.55 m <sup>2</sup> / 11.49 s	12.50 m <sup>2</sup> / 12.46 s	12.67 m <sup>2</sup> / 13.18 s	13.03 m <sup>2</sup> / 14.99 s
Cruise490PAX	12.48 m <sup>2</sup> / 15.60 s	13.32 m <sup>2</sup> / 16.56 s	14.19 m <sup>2</sup> / 17.65 s	14.83 m <sup>2</sup> / 18.46 s	17.10 m <sup>2</sup> / 20.49 s
Cruise977PAX	8.56 m <sup>2</sup> / 10.65 s	8.90 m <sup>2</sup> / 11.50 s	9.34 m <sup>2</sup> / 12.47 s	9.73 m <sup>2</sup> / 13.20 s	10.56 m <sup>2</sup> / 15.02 s
ExpCruisePods	3.59 m <sup>2</sup> / 16.87 s	4.01 m <sup>2</sup> / 18.14 s	4.12 m <sup>2</sup> / 19.61 s	4.38 m <sup>2</sup> / 20.70 s	8.80 m <sup>2</sup> / 23.44 s

## Conclusions

The presented estimation is as accurate as possible within the limited resources. Objections against the taken simplifications and assumptions will have to take into account that individual resistance astern and propulsion tests, four-quadrant propeller tests at all pitch angles, questionnaires for engine manufacturers and expensive data mining and literature studies are not within the scope of this task.

As the ship bow was assumed to penetrate the other ship hull one should question, whether the bow is initially exposed to the same hydrostatic pressure as the rest of the hull. If it is, then the damaged compartment of the opposite ship should be flooded already and in principle no further water will enter the struck ship and cause a roll moment. If it is not, then the resistance should initially be increased by the corresponding force. Such information is not available and it is expensive to determine. Further, it is not easy to find out how this initial hydrostatic pressure and additional resistance decay, when the ship is retracting its bow out of the damage. We assume that this effect decays very fast and neglect it.

## References

- [1] Robert F. Roddy, David E. Hess, and Will Faller. Neural network predictions of the 4-quadrant Wageningen propeller series. Report NSWCCD-50-TR-2006/004, David Taylor Model Basin, Naval Surface Warfare Center, Carderock Division, West Bethesda, Maryland, April 2006.

## 7.7 Annex G: Leakage and collapse of non-watertight structures

(Author: Dr. Pekka Ruponen, NAPA)

The watertight compartments of passenger ships are usually further subdivided into smaller rooms with non-watertight decks and bulkheads. Some typical examples are illustrated in Figure 4-7 below. These structures can have a notable effect on the flooding progression, and subsequently also on the stability of the damaged ship. The real flooding sequence can only be calculated with time-domain simulation, where the leakage and collapse of the non-watertight structures is reasonably accounted for.

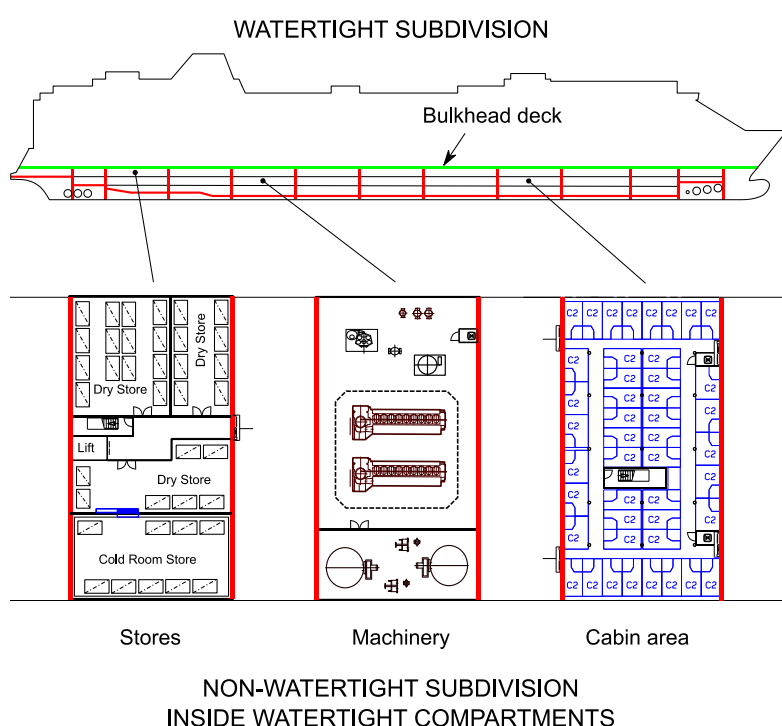


Figure 7-10 Watertight subdivision of a passenger ship with three examples of non-watertight subdivision in some WT compartments, adopted from Jalonen et al. (2017)

Leakage and collapse of non-watertight doors, and their effects on the flooding progression in time-domain, were first discussed by van 't Veer et al. (2004). However, since neither experimental data nor numerical studies were available, educated guesses were used for leakage and collapse parameters of different door types, as presented in SLF47/INF.6. These early studies were motivation for the EU FP7 project FLOODSTAND, where research focused on both full-scale experiments and numerical analyses on leakage and collapse characteristics of various typical non-watertight structures in passenger ship. An extensive summary of the tests, calculations and analyses is presented in Jalonen et al. (2017). Detailed description of the measurements is given in Jakubowski and Bieniek (2010), and the Finite Element analyses are presented by Naar and Vaher (2011).

The following paragraphs provide a brief summary of the observed leakage and collapse mechanisms for typical non-watertight structures in passenger ships, based on the FLOODSTAND results.

### Leakage and collapse mechanisms

When a non-watertight structure is subjected to floodwater pressure, it will either leak or collapse, depending on the effective pressure. In this section, the leakage and collapse mechanisms are discussed, based on the research in the EU FP7 project FLOODSTAND.

In the full-scale tests, the A-class steel bulkheads did not suffer notable damage under the water pressure. This confirmed the assumption in SLF47/INF.6 that the steel bulkheads can be considered watertight if the leakage and collapse of doors is properly taken into account.

The process of leakage and collapse for a closed non-watertight door in a steel bulkhead is illustrated in **Error! Reference source not found.**, namely:

- With very small pressure heads, it is possible that there is no leakage, and the door actually prevents progressive flooding
- With increased water pressure head the door is deformed and leaking starts, or is increased
- When a critical pressure head is reached the door collapses

The leakage and collapse characteristic can be notably different depending on the direction of the water pressure and the opening direction of the door. In this respect, the directions are defined as “into” and “out from” the doorframe. A schematic illustration of a non-watertight door in a bulkhead is presented in **Error! Reference source not found.**, clarifying this terminology.

There is often a small gap between the bottom of the door and the sill. The size of this gap has a very significant effect on the leaking rate. Therefore, it is also very likely that different doors of the same type can have different leakage properties, even on the same ship.

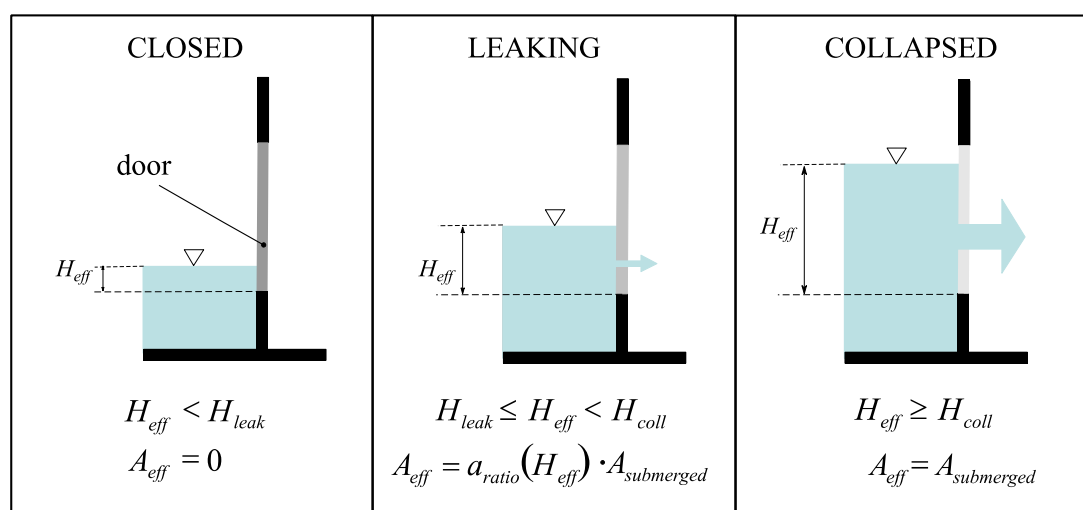


Figure 7-11 Effective area of a closed non-watertight door in different conditions under the pressure of floodwater, Jalonen et al. (2017)

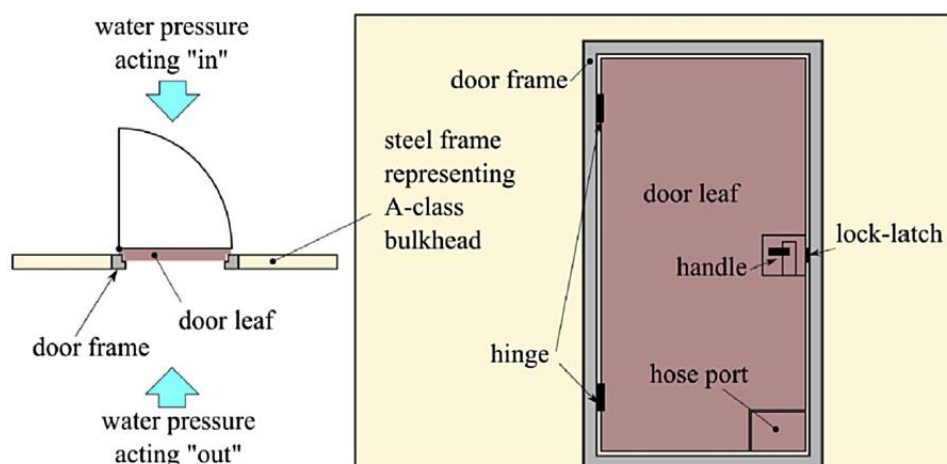


Figure 7-12 Schematic drawing of a hinged single leaf door and the directions for the pressure of the floodwater, Jalonen et al. (2017)

In addition to the measurement data, also the videos and photos on the damage to the tested structures were very useful in increasing the knowledge on the leakage and collapse mechanisms. **Error! Reference source not found.** shows notable leakage in the test of a hinged A-class fire door. The door is deformed, and water sprays especially beneath the door. Some details of the failure mechanisms for this door type are visualized in **Error! Reference source not found.**. In general, the lock latch and the hinges are considered the weak points for the collapse of the door.



Figure 7-13 Hinged A-class fire door under 12 kPa water pressure; notable leakage, photo adopted from Jakubowski and Bieniek (2010)

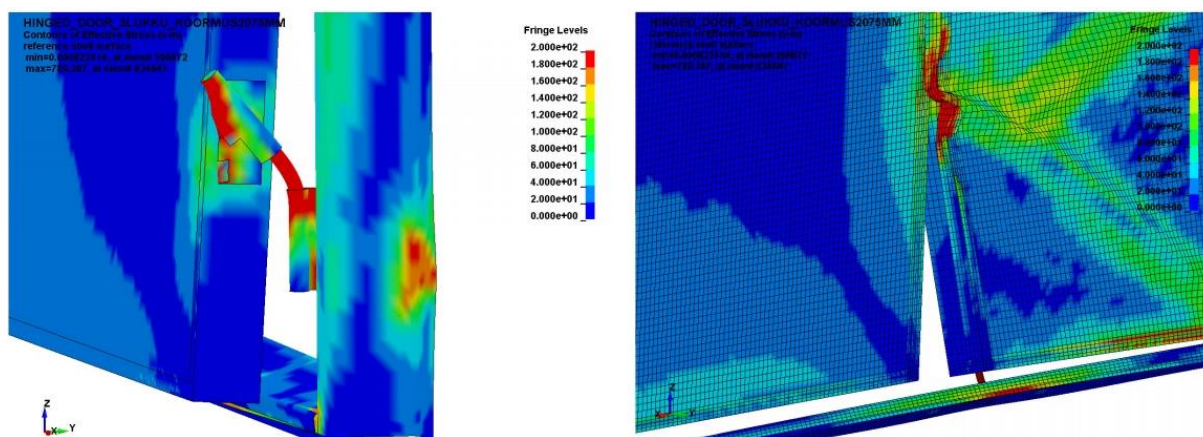


Figure 7-14 Details from the FE analyses visualizing the failure mechanisms of hinged A-class fire doors, Naar and Vaher (2011)

### FLOODSTAND approach to model leakage and collapse

Based on the results, an enhanced simplified model was developed for leakage and collapse of doors to be used in time-domain flooding simulation. The same three parameters, already introduced in SLF47/INF.6, were used:

- leakage threshold pressure head,  $H_{leak}$
- leakage area ratio,  $a_{ratio}$
- collapse threshold pressure head,  $H_{coll}$

The leakage area ratio is defined as:

$$a_{ratio} = \frac{A_{leaking}}{A_{submerged}}$$

where  $A_{leaking}$  is the area of the door that is leaking and  $A_{submerged}$  is the total submerged area of the door.

Leakage is a result of possible gaps between the door and the doorframe, and most notably deformation of the structures under the water pressure. The deformation may be increased as a function of the effective pressure head. Consequently, the following linear equation was applied:

$$a_{ratio} = \alpha + \beta H_{eff}$$

It was found out in the analysis of the FLOODSTAND test results that either the constant  $\alpha$  or the slope coefficient  $\beta$  was zero for all tested door types. Consequently, the leakage area ratio was either:

- constant or
- linearly increasing from zero value

The recommendations, derived from the full-scale tests and FE analyses, are summarized in **Error! Reference source not found.**

The pressure of the floodwater results in permanent deformation of the non-watertight structures. Therefore, the leakage area ratio cannot decrease, even if the effective pressure

on the door decreases. This means that the simulation program needs to track the applied leakage area ratio for each door, and update this value at each time step, if the effective pressure height has increased, Ruponen (2017). However, it should be noted that this approach is not fully valid for doors with a hose port since the port may be closed if the pressure acting on the door decreases.

Table 7.1 Summary of the FLOODSTAND recommendations for leakage & collapse modelling of different door types, Jalonen et al. (2017)

Door type	Pressure direction	$H_{leak}$ [m]	$\alpha_{ratio} = \alpha + \beta H_{eff}$		$H_{coll}$ [m]	Note
			$\alpha$ [-]	$\beta$ [1/m]		
A-class hinged (single leaf)	into	0.0	0.0	0.02	2.5	Doors with a hose port can have larger leakage at lower pressure heads, but for simplicity, the same guideline values can be used.
	out	0.0	0.0	0.03	2.5	
A-class double leaf	out	0.0	0.025	0.0	2.0	Collapsing pressure head based on FE analysis
A-class sliding	into	0.0	0.025	0.0	1.0	
	out	0.0	0.025	0.0	1.0	
Cold room sliding door	into	0.0	0.0	0.03	3.5	Collapsing pressure head based on FE analysis
B-class joiner door	into	0.0	0.0	0.03	1.5	Panels around the door will fail first, thus leakage area is very approximate
	out	0.0	0.03	0.0	1.5	

### B-class fire rated structures

Some photos from the tests with B-class fire rated structures are shown in **Error! Reference source not found.** Based on the test results, the following summary on the B-class boundaries was presented in Jalonen et al (2017):

“For the B-class wall panels the maximum pump capacity was reached with a moderate pressure head of about 1.2 m. The numerical analyses, Naar and Vaher (2011), support this observation. For the wall panels that had steel frames, the leakage was much smaller when the pressure was acting towards the frame. “

“Based on these test results, the B-class structures do restrict the flow of floodwater, but not significantly. Moreover, since also the walls are seriously damaged, even under moderate pressure heads, the results confirm the simplified approach in SOLAS II-1 that the B-class structures can be excluded in the calculation of intermediate flooding stages.”

However, B-class joiner doors that are fitted into steel bulkheads should be modelled for time-domain simulation of progressive flooding.



Figure 7-15 B-class fire rated structures in FLOODSTAND tests, damage to wall around a closed door (left) and significant leaking of a wall (right), photos adopted from Jakubowski and Bieniek (2010)

### Other research on collapse of doors under water pressure

Recently, also Wells et al. (2019) have published tests results for collapse of non-watertight doors under water pressure. In this study, the focus was on doors used in nuclear power plants. Two different door types were tests:

- wooden hollow core, outward swinging doors and
- steel, inward swinging doors

In principle, it can be assumed that the steel door is somewhat similar to the doors used on ships, and therefore these results are compared to the FLOODSTAND results.

Some photos from the tests by Wells et al. (2019) are shown in **Error! Reference source not found..** When pressure is acting outwards from the doorframe, the locking device failed and the door was practically “opened” by the water pressure. With pressure acting into the doorframe,

notable deformation took place. The average “failure depth” for outward direction was 0.90 m, and changing the steel door orientation (pressure into the doorframe) increased the failure depth to 2.05 m.



Figure 7-16 Tests on a steel door, with outward pressure (left) and inward pressure (right), photos adopted from Wells et al. (2019)

In the FLOODSTAND tests for A-class single leaf hinged doors the collapse pressure head was about 2.5 m for both pressure directions. The notable difference in the results for outward pressure case (0.90 m and 2.5 m) could be explained by different lock latch arrangement. It should be noted that the maximum pumping capacity of the facility was reached in corresponding FLOODSTAND door test, and the collapse pressure head for this case is based on FE analysis.

For the case with pressure acting into the doorframe, the results of the two tests are quite close to each other (2.05 m and 2.5 m). Unfortunately, the leakage rate was not measured and reported by Wells et al. (2019).

### Sensitivity of time-to-flood to leakage and collapse parameters

A study on the effects of random variation in the leakage and collapse parameters for closed non-watertight doors has been presented in Ruponen (2017). The effects of collapse pressure head and leakage area were studied separately for two damage scenarios, and each case was repeated 250 times with random door parameters, **Error! Reference source not found..** Examples of the simulation results are presented in **Error! Reference source not found.** and **Error! Reference source not found..** There were certain critical doors for progressive flooding, and if these doors collapsed sooner, the time-to-capsize was notably shorter. The leakage area ratio had less dramatic effects.

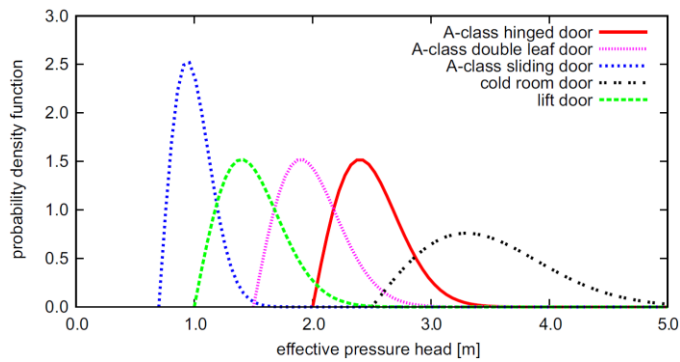


Figure 7-17 Example of applied probability density functions for the collapse pressure head of different door types, Ruponen (2017)

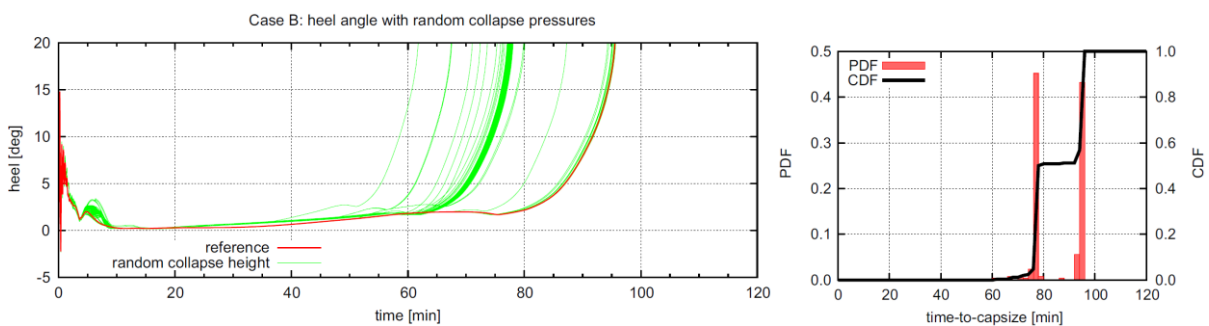


Figure 7-18 Example of simulation results with random collapse pressures, Ruponen (2017)

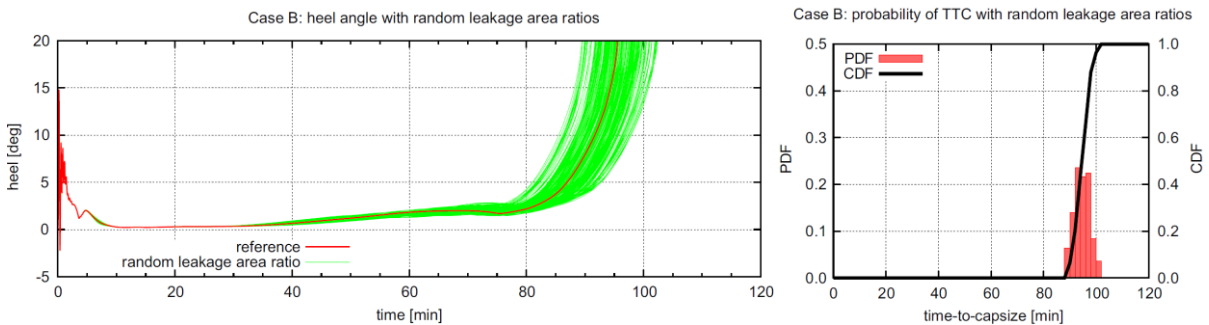


Figure 7-19 Example of simulation results with random leakage area ratio, Ruponen (2017)

## Summary

Leakage and collapse of non-watertight structures is a major cause for progressive flooding, especially in passenger ships with several A-class fireproof subdivision within the watertight compartments.

Recommendation for modelling leakage and collapse of various typical door types have been derived based on the full-scale tests and FE analyses within the EU FP7 project FLOODSTAND. These parameters have become an “industry standard”. However, the comparison of the results from FLOODSTAND and Wells et al. (2019) demonstrates that the details of the door structure and fitting to the surrounding bulkhead can have a notable effect on the leakage and collapse characteristics.

Variation in the actual leakage area ratio and critical collapse pressure head will inevitably mean uncertainty in the simulation results, most notably for the time-to-flood/capsize, as presented in Ruponen (2017). Consequently, further tests and FE analyses on different typically used doors would be extremely valuable. However, the FLOODSTAND recommendations are the state-of-the-art, and considered suitable for flooding simulations, both for design and operation of ships. Yet, the uncertainties should be taken into account in the analysis of the simulation results.

## References

Jakubowski, P., Bieniek, N. 2010. Experiments with leaking and collapsing structures. FLOODSTAND Deliverable D2.1b. Other report identifications: CTO S.A. RK, No. RK-2010/T-052 /E, CTO reference: 5.167.01.221.

[http://floodstand.aalto.fi/Info/Files/FLOODSTAND\\_Deliverable\\_D2.1b\\_final\\_v.1.6.pdf](http://floodstand.aalto.fi/Info/Files/FLOODSTAND_Deliverable_D2.1b_final_v.1.6.pdf)

Jalonen, R., Ruponen, P., Weryk, M., Naar, H. and Vaher, S. 2017. A study on leakage and collapse of non-watertight ship doors under floodwater pressure, *Marine Structures*, Vol. 51, pp. 188-201. <http://dx.doi.org/10.1016/j.marstruc.2016.10.010>

Naar, H., Vaher, S. 2011. Numerical study on the critical pressure heads. FLOODSTAND Deliverable 2.2a.

[http://floodstand.aalto.fi/Info/Files/FLOODSTAND\\_Deliverable\\_D2.2a\\_final\\_v.2.pdf](http://floodstand.aalto.fi/Info/Files/FLOODSTAND_Deliverable_D2.2a_final_v.2.pdf)

Ruponen, P. 2017. On the effects of non-watertight doors on progressive flooding in a damaged passenger ship, *Ocean Engineering*, Vol. 130, pp. 115-125. <http://dx.doi.org/10.1016/j.oceaneng.2016.11.073>

SLF47/INF.6 2004. Large Passenger Ship Safety: Survivability Investigation of Large Passenger Ships, submitted by Finland, 11th June 2004.

Van 't Veer, R., Peters, W., Rimpelä, A-L., de Kat, J. 2004. Exploring the Influence of Different Arrangements of Semi-Watertight Spaces on Survivability of a Damaged Large Passenger Ship, *Proceedings of the 7th International Ship Stability Workshop*, Shanghai, China, 1-3. November 2004.

Wells, A., Ryan, E.D., Savage, B., Tahhan, A., Suresh, S., Muchmore, C., Smith, C.L, Pope, C.L. 2019. Non-watertight door performance experiments and analysis under flooding scenarios, *Results in Engineering*, Vol. 3, article 100031. <https://doi.org/10.1016/j.rineng.2019.100031>